

# EVALUATION OF CONTAINMENT LINER PLATE LEAK CHASE CHANNEL SYSTEM

FOR  
POINT BEACH NUCLEAR PLANT  
UNITS 1 & 2

J.V. Rotz  
M. Reifschneider

Bechtel Associates Professional Corporation



8608040108 860724  
PDR ADOCK 05000266  
P PDR

81-03417

EVALUATION OF CONTAINMENT LINER PLATE  
LEAK CHASE CHANNEL SYSTEM

FOR

POINT BEACH NUCLEAR PLANT  
UNITS 1 AND 2

by: J.V. Rotz  
M. Reifschneider

Bechtel Associates Professional Corporation  
June 1986



EVALUATION OF CONTAINMENT LINER PLATE  
LEAK CHASE CHANNEL SYSTEM

FOR

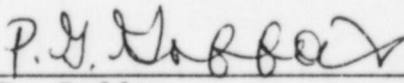
POINT BEACH NUCLEAR PLANT  
UNITS 1 AND 2

Prepared by:

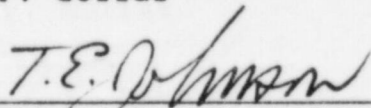
  
\_\_\_\_\_  
J.V. Rotz

  
\_\_\_\_\_  
M. Reifschneider

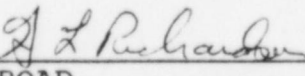
Reviewed by:

  
\_\_\_\_\_  
P. Goffas

Approved by:

  
\_\_\_\_\_  
T.E. Johnson

Concurrence by:

  
\_\_\_\_\_  
H.A. ABLONDI  
PQAD

Bechtel Associates Professional Corporation  
June 1986

EVALUATION OF CONTAINMENT LINER PLATE  
LEAK CHASE CHANNEL SYSTEM

FOR

POINT BEACH NUCLEAR PLANT  
UNITS 1 AND 2

TABLE OF CONTENTS

	<u>Page</u>
1.0 <u>INTRODUCTION</u>	1-1
2.0 <u>SUMMARY</u>	2-1
2.1 RESULTS	2-1
2.2 GENERAL ASSESSMENT	2-3
3.0 <u>PERFORMANCE HISTORY</u>	3-1
4.0 <u>QUALITY VERIFICATION OF CONSTRUCTION RECORDS</u>	4-1
4.1 GENERAL	4-1
4.2 MATERIALS VERIFICATION	4-1
4.3 LEAK CHASE SYSTEM TESTING	4-2
4.4 WELDING OF LCCs TO LINER PLATE	4-2
5.0 <u>LINER PLATE LCC SYSTEM DESCRIPTION AND BEHAVIOR</u>	5-1
5.1 BACKGROUND	5-1
5.2 GENERAL CONFIGURATION	5-1
5.2.1 Test Pipes and Tubing	5-4
5.3 STRUCTURAL BEHAVIOR AND ANALYTICAL APPROACH	5-5
5.3.1 Plate Curvature	5-6
5.3.2 Exterior LCCs (Dome Section)	5-6
5.3.3 Interior LCCs	5-8
5.4 MATERIALS PROPERTIES	5-9
5.4.1 Liner Plate and LCC Components	5-9
5.4.2 Concrete	5-10
6.0 <u>LOADS</u>	6-1

Table of Contents (Continued)

	<u>Page</u>
7.0 <u>EMBEDDED LCC SECTION ANALYSIS</u>	7-1
7.1 SECTION SELECTION	7-1
7.2 MATHEMATICAL MODEL	7-2
7.3 MODEL SOLUTION	7-4
7.4 LOAD CASES	7-5
7.5 RESULTS OF ANALYSES	7-7
8.0 <u>INTERIOR LCC SECTION ANALYSES</u>	8-1
8.1 LCC SECTION SELECTION	8-1
8.2 LOADING CONDITIONS	8-1
8.3 ANALYTICAL APPROACH	8-2
8.4 RESULTS OF ANALYSES	8-4
8.5 BASE LCC SECTION CLEARANCE CHECK	8-5
8.6 TEST PIPES	8-6
8.6.1 Test Pipes for Exterior LCCs	8-6
8.6.2 Test Pipes for Interior LCCs	8-7
9.0 <u>LEAKTIGHT INTEGRITY</u>	9-1
10.0 <u>OVERALL ASSESSMENT</u>	10-1
10.1 PERFORMANCE HISTORY	10-1
10.2 QUALITY OF CONSTRUCTION	10-2
10.3 STRUCTURAL EVALUATION	10-3
10.4 LEAKTIGHT INTEGRITY	10-3
10.5 CONCLUSION	10-4
11.0 <u>REFERENCES</u>	11-1

APPENDIXES

A	Notation
B	Liner Plate Leak Chase Channel Tests

Table of Contents (Continued)

LIST OF TABLES

3-1	Summary of Data for Operating Plants with Similar Liner Plates (References 2 and 3)
4-1	Summary of Referenced Construction Documents
5-1	Location and Description of Internal LCC Sections
5-2	Liner Plate and LCC Element Physical Properties
5-3	Concrete Physical Properties
7-1	Spring Element Properties
7-2	Parametric Evaluation Matrix
7-3	Element Loads and Displacements (Cases 1 - 7)
7-4	Comparison of Maximum Element Response Values with Capacities for Case 1
7-5	Comparison of Maximum Element Response Values with Capacities for Case 2
7-6	Comparison of Maximum Element Response Values with Capacities for Case 3
7-7	Comparison of Maximum Element Response Values with Capacities for Case 4
7-8	Comparison of Maximum Element Response Values with Capacities for Case 5
7-9	Comparison of Maximum Element Response Values with Capacities for Case 6
7-10	Comparison of Maximum Element Response Values with Capacities for Case 7
7-11	Comparison of Maximum LCC Element Response Values with Capacities for Cases 1 - 5 & 7
8-1	Summary of Interior LCC Section Analyses
B2-1	Test Component Legend
B2-2	Specimen Strength Properties
B2-3	Summary of First Observed Crack and Ultimate Load and Displacement Data for Composite Tests



Table of Contents (Continued)

List of Tables (Continued)

- B2-4 Shear Load Versus Displacement Data for Composite Test Specimens
- B2-5 Summary of Shear Load Versus Displacement Data for the Independent Steel Liner Plate LCC Tests
- B3-1 LCC Bilinear Spring Properties

LIST OF FIGURES

- 5-1 Liner Plate Locations
- 5-2 Dome Liner Plate Section and Details
- 5-3 Typical Cylindrical Shell Sections
- 5-4 Leak Chase Channel and Seal Weld Location in Base Liner Plate
- 5-5 Typical Leak Chase Channel Detail in Base Slab
- 5-6 Typical Interior LCC Sections
- 7-1 Mathematical Model for Dome Liner Plate Section
- 7-2 Resistance Functions for Liner Plate Component Springs
- 8-1 Typical LCC Loading and Models
- 8-2 Location of Base Liner Plate Controlling Section
- B2-1 Composite Liner Plate LCC Specimen
- B2-2 Independent Steel Liner Plate Leak Chase Channel Specimen
- B2-3 Composite Specimen Test Assembly including Pneumatic and Hydraulic Systems
- B2-4 Test Assembly Including Pneumatic System and Dial Gage Arrangement for Independent Steel Specimen Tests
- B3-1 Combined Plot of Composite Test Data for all Tests up to Maximum Load
- B3-2 Combined Plot of Load vs. Displacement Data for Independent Steel Liner Plate LCC Tests

EVALUATION OF CONTAINMENT LINER PLATE  
LEAK CHASE CHANNEL SYSTEM

1.0 INTRODUCTION

This investigation was undertaken to assess the ability of the liner plate leak chase channel (LCC) system to function as an integral part of the containment structure leaktight pressure boundary. This investigation included the following:

- a. A survey of performance history for liner plates and LCCs with respect to development of inservice leaks in other plants
- b. Evaluation of construction records for the Point Beach liner plate system with respect to material verification and quality control
- c. Structural analyses of typical containment liner plate sections to evaluate the severity of loading on LCCs.
- d. Executing a test program to define the load-displacement characteristics of LCCs (interacting with the liner plate and containment concrete) and to verify the leaktight integrity of the LCCs while subjected to extreme load and displacement conditions.

## 2.0 SUMMARY

### 2.1 RESULTS

The results of this investigation are summarized as follows:

- a. Historically, no evidence of unacceptable leakage was found for LCCs or liner plate butt welds in United States (US) plants subsequent to the initial (before startup) integrated leak rate test (ILRT).

Plants (US) with liner plate systems similar to Point Beach represent a population of at least 49 (22 of these are Bechtel-designed plants). These plants represent over 400 reactor years of operating experience and over 100 ILRTs (subsequent to the initial ILRT) with no apparent liner plate or LCC leakage. For further details, see Section 3.0.

- b. The specified verification of materials, inspections, testing, and other quality control requirements for the LCCs are similar to those for other components of the liner plate system.

A review of construction records for Point Beach indicates that the liner plate system (including LCCs) has been fabricated, constructed, and tested in accordance with specified requirements. For further discussion, see Section 4.0.

- c. Several sections of the liner plate system (typical of conditions in the base, cylinder, and dome areas) were selected and analyzed. These analyses indicate that some of the LCC sections in the cylinder portion of the containment could sustain minor inelastic deformations when subjected to maximum design load conditions. Most

would remain elastic (see Section 8.0). The dome area LCCs, which are embedded in concrete, would also sustain some nonlinear deformation with a minimum safety factor with respect to available strain energy capacity of about 11. This is well within the acceptable range (greater than 2). The presence of accident pressure of 60 psi increased this safety factor to 16.6. The lowest safety factor for interior LCCs at other locations was 22 (based on displacement). For further description and discussion of the analyses, see Sections 7.0 and 8.0.

- d. In addition to providing the load-displacement properties of the LCCs embedded in concrete (utilized in the analyses), the test program demonstrated the strength and leaktight integrity of the LCCs. For the composite tests (LCC embedded in concrete), the shear resistance capacity was controlled by compressive failure of the concrete engaged by the LCC. For the liner plate LCC (steel only) tests, the capacity was limited by the flexural resistance of the 1/4-inch thick liner plate. Although the sections sustained considerable inelastic displacement in these tests (in excess of 0.10 inch), no failures were observed in the channels or their welds to the liner plate. Leaktight integrity of the LCCs was maintained through completion of all tests.

The maximum calculated displacement of the exterior embedded dome LCCs was only 3.2% of the measured displacement producing no leaks. The maximum calculated angular displacement (rotation) of interior LCC elements was 1.7% of the measured rotation (at weld) producing no leaks. For further discussion, see Section 9.0.



## 2.2 GENERAL ASSESSMENT

The analyses show that the stress and displacement levels of the LCCs associated with the most severe postulated loading conditions on the liner plate system, are well within acceptable limits which have been verified experimentally. The presence of the LCC has a general beneficial effect on the remaining elements of the liner plate system (loads taken by an LCC relieves loads required to be taken by other elements). For example, the presence of the LCC raises the minimum safety factor of the anchor angle elements from 6.6 to 10.8 (Case 6 versus Case 1, Section 7.5).

The LCC is not a weak link in the liner plate system. The capacity of the liner plate system is controlled by failure or excessive displacement of other elements in the system (while the leaktight integrity of the LCCs is maintained).

Specifications required and construction records document that all LCC sections were leak tested during construction to a minimum of 70 psig. Therefore, the leak tightness of the LCC and liner plate welds has been verified.

The foregoing analyses and testing, along with a favorable performance history for Point Beach and similar liner plate systems, and documented quality assurance during construction, indicates that the LCC system can reliably function as a part of the containment structure liner plate pressure boundary.

### 3.0 PERFORMANCE HISTORY

The performance history of the liner plate systems for Point Beach Units 1 and 2 has been uneventful in 12 to 14 years of operation. The experience of other plants with similar liner plate systems has been comparable.

Knowledgeable personnel from Bechtel and Sargent & Lundy (S&L) were contacted to summarize performance of their respective plants. (This involved 22 Bechtel plants and four S&L plants.)

Some of the plants (such as Maine Yankee, Beaver Valley 1, and Zion 1 and 2) have containment liner plates that are fully leak chased similar to Point Beach. Most of the others are partially leak chased (usually in areas with difficult accessibility).

No history of LCC or liner plate leaks subsequent to the initial ILRT was reported.

An inquiry made through INPO (Institute of Nuclear Power Operations) regarding reported leaks in LCCs or liner plates subsequent to initial ILRTs also revealed no reported history of leaks.

Other plants having containment liner plate systems similar to that of Point Beach Units 1 and 2 are identified in Table 3-1 (References 2 and 3). In addition, the design architect engineer (A/E), reactor type, containment type, date of commercial operation, and years of operation are indicated.

A reduction of the operating history data given in Table 3-1 indicates that a total of approximately 400 reactor years of operating experience has been accumulated for the 49 plants with similar liner plate designs.

Reference 6 (10 CFR 50 Appendix J) requires an initial ILRT and an average of three ILRTs for each 10 years of operation. From this and the data in Table 3-1, it is estimated that about 150 ILRTs have been performed, over 100 of these have been performed after commencement of commercial operation with no significant liner plate leakage.

This demonstrates that liner plate systems such as those installed at Point Beach are historically reliable and troublefree.

TABLE 3-1 - SUMMARY OF DATA FOR OPERATING PLANTS WITH SIMILAR LINER PLATES  
(REFERENCES 2 AND 3)

Plant	A/E	Reactor Type	Containment Type	Date Commercial (mo/yr)	Years Operating	Remarks
Arkansas Nuclear One-1	B	PWR	3b	12/74	11.1	
Arkansas Nuclear One-2	B	PWR	3b	03/80	5.8	
Beaver Valley-1	S&W/B&R	PWR	3d	04/77	8.7	Full leak chase
Brunswick-1	UE&C	BWR	5g MK II	03/77	8.8	
Brunswick-2	UE&C	BWR	5g MK II	11/75	10.1	
Calvert Cliffs-1	B	PWR	3b	05/75	10.6	
Calvert Cliffs-2	B	PWR	3b	04/77	8.7	
Connecticut Yankee	S&W	PWR	3	01/68	18.0	
Cook-1	AEPSC	PWR	3c	08/75	10.4	
Cook-2	AEPSC	PWR	3c	07/78	7.5	
Crystal River-3	Gilbert	PWR	3b	03/77	8.8	
Farley-1	B	PWR	3b	12/77	8.1	
Farley-2	B	PWR	3b	07/81	4.5	
Fort Calhoun-1	GHD&R	PWR	3b	09/73	12.3	
Ginna	Gilbert/B	PWR	3a	03/70	15.8	
Indian Point-1	Utility	PWR	3	07/74	6.0	Retired 1980
Indian Point-2	UE&C	PWR	3	08/76	9.4	
La Salle County-1	S&L	BWR	5g (MK II)	10/82	3.2	
La Salle County-2	S&L	BWR	5g (MK II)	06/84	1.6	
Maine Yankee	S&W	PWR	3	12/72	13.1	Full leak chase
McGuire-1	Utility	PWR	3c	12/81	4.1	
McGuire-2	Utility	PWR	3c	03/84	1.8	
Millstone-2	B	PWR	3bf	12/75	10.1	
North Anna-1	S&W	PWR	3d	06/78	7.6	
North Anna-2	S&W	PWR	3d	12/80	5.1	
Oconee-1	B	PWR	3b	07/73	12.5	
Oconee-2	B	PWR	3b	09/74	11.3	
Oconee-3	B	PWR	3b	12/74	11.1	
Palisades	B	PWR	3b	12/71	14.1	
Point Beach-1	B	PWR	3b	12/70	15.1	Full leak chase
Point Beach-2	B	PWR	3b	10/72	13.2	Full leak chase
Rancho Seco-1	B	PWR	3b	04/75	10.7	
Robinson-2	Ebasco	PWR	3a	03/71	14.8	



Table 3-1 (Continued)

Plant	A/E	Reactor Type	Containment Type	Date Commercial (mo/yr)	Years Operating	Remarks
Salem-1	Utility	PWR	3	06/77	8.6	
Salem-2	Utility	PWR	3	10/81	4.2	
San Onofre-2	B	PWR	3b	08/83	2.4	
San Onofre-3	B	PWR	3b	04/84	1.7	
Summer	Gilbert	PWR	3b	01/84	2.0	
Surry-1	S&W	PWR	3d	12/72	13.1	
Surry-2	S&W	PWR	3d	05/73	12.6	
Susquehanna-1	B	BWR	5g MK II	06/83	2.6	
Susquehanna-2	B	BWR	5g MK II	01/85	1.0	
Three Mile Island-1	Gilbert	PWR	3b	09/74	11.3	
Trojan	B	PWR	3b	05/76	9.6	
Turkey Point-3	B	PWR	3b	12/72	13.1	
Turkey Point-4	B	PWR	3b	09/73	12.3	
Zion-1	S&L	PWR	3b	12/73	12.1	Full leak chase
Zion-2	S&L	PWR	3b	09/74	11.3	Full leak chase

LEGEND

Abbreviations:

AEPSC	American Electric Power Service Corp.
B	Bechtel
B&R	Burns & Roe
Ebasco	Ebasco Services, Inc.
GHD&R	Gibbs, Hill, Durham & Richardson, Inc.
Gilbert	Gilbert Associates, Inc.
S&L	Sargent & Lundy
S&W	Stone & Webster Engineering Corp.
SCSI	Southern Company Services, Inc.
UE&C	United Engineers & Constructors, Inc.

Table 3-1 (Continued)

Containment Type:

Containment Type 3      Reinforced concrete cylinder with steel liner  
Pressure Suppression Type 5      Reinforced concrete drywell and wet well with steel liner

Features

- a    Post-tensioned vertically only
- b    Post-tensioned in three directions
- c    Ice condenser
- d    Subatmospheric
- f    Secondary containment, steel enclosure building, for Type 3
- g    Secondary containment, concrete and/or steel, for Types 4, 5, and 6

#### 4.0 QUALITY VERIFICATION OF CONSTRUCTION RECORDS

##### 4.1 GENERAL

Verification of existing construction records included reviewing documents identified in Table 4-1. The results of this review indicate that the construction of the liner plate and LCCs agrees with the specification requirements (Reference 7) and that the quality requirements for the LCCs were similar to those for the other liner plate components. Verification included a review of the existing records at the Point Beach nuclear plant and the records maintained by Bechtel's Ann Arbor Area Office.

##### 4.2 MATERIALS VERIFICATION

A comparison was made between the relevant Graver liner plate and LCC drawings listed in Table 4-1, the bills of material and the available material certifications. In all cases, the material certifications and fabrication drawings were found to be in agreement with the specified material requirements. The available records do not provide full coverage of all the liner plate material. Typically, material certifications were available for some, but not all of a particular component material. In one case, no certification for a component material was found (weld filler material). The fabrication drawings did, however, call out the proper specified weld filler material. This indicates that the proper filler material was used. The available records are, therefore, considered representative of the liner plate and LCC materials and provide confirmation that the liner plate and LCC materials conform to Specification 6118-C-7, Section 15.0. (Reference Table 4-1, Item C.)

No nonconformances or approved material substitutions were noted in the review of certifications.

#### 4.3 LEAK CHASE SYSTEM TESTING

The construction field sketches (FSKs) identified in Table 4-1 show that the LCCs (and other leak chase system components) were successfully 100% pressure-tested in accordance with Subsection 17.2.2 of Specification 6118-C-7 (Reference 7) after the liner plate welds were vacuum box tested. The FSKs identify completed welds, the location of the welds, and the boundaries and results of pressure tests for the LCCs.

#### 4.4 WELDING OF LCCs TO LINER PLATE

Welding of the LCCs to the liner plate was specified to be a 3/16-inch double pass fillet weld in accordance with AWS D1.0-63, applicable Graver drawings, and shop and field specifications. The above-referenced FSKs identify the welders of the LCCs and the weld locations. Documentation of welder qualifications was not retained in the records.



TABLE 4-1 - SUMMARY OF REFERENCED CONSTRUCTION DOCUMENTS

A. GRAVER<sup>(1)</sup> DRAWINGS

L23672-2  
L23481-0  
L23482-0  
L23499A-0  
L23674-1  
L23484-0  
L23485-2  
L23487-2  
L23675-0  
L24138F-0  
L23486A-2  
L23684-1  
L23660-1  
L23659-1  
L23460-0  
L23459-1  
L23480-0  
L23458-2  
L23476Z-4  
L23483-0  
L23690E-1  
L23490E-1  
L23680-1  
L23681-1  
L23683-1  
L23658-1  
L23682-1  
L23691-2  
L23491-3

B. CONSTRUCTION FSKs

(Liner plate welding roll out)<sup>(2)</sup>  
FSK-6118-CV-194-SH2  
FSK-6118-CV-194-SH1  
FSK-6118-CV-194-SH5  
FSK-6118-CV-194-SH4  
FSK-6119-CV-194-SH3

---

(1) Graver Tank and Manufacturing Company, liner plate fabricator

(2) Included radiographic, vacuum box, and pressure tests of groove welds and LCC welds.

Table 4-1 (Continued)

C. MATERIAL CERTIFICATION

<u>Material</u>	<u>Component</u>
ASTM A 36	LCC and 3 x 2 anchor angles
ASTM A 442 Gr. 60	1/4 inch liner plate
ASTM A 516 Gr. 70	Thickened liner plate
ASTM A 283 Gr. C	Structural shape

Specifications, Codes, Standards

Specification/Requisition 6118-C-7, Rev 3  
AWS D1.0.63, "Structural Welding Code"  
ASTM Part 4 1969 Ed.

## 5.0 LINER PLATE LCC SYSTEM DESCRIPTION AND BEHAVIOR

### 5.1 BACKGROUND

The LCC system is an integral part of the liner plate system which forms the pressure boundary on the inside surface of the containment structure. The LCCs are formed by welding steel channel, angle, plate, or split pipe sections over butt welds joining liner plate sections together or over welds at intersections of penetrations or other openings through the liner plate. The initial purpose of the LCCs was to provide a means to pressure test the liner plate or penetration welds for leaks.

Construction specifications (Reference 7) also required that these channels and their welds be tested to confirm leaktight integrity. This resulted in a fully leak tested redundant pressure boundary in the areas bounded by the LCCs.

The original liner plate analysis and design considered only the liner plate and its anchorage system for structural and leaktight integrity. No structural or other benefits were taken for the LCC system and, as a consequence, the LCCs were not included in any structural testing or analysis. Therefore, additional analyses and tests, as described herein, were performed to demonstrate both structural and leaktight integrity of the LCC system.

### 5.2 GENERAL CONFIGURATION

The general configuration of the liner plate system, along with identification of major liner plate areas, is shown in Figure 5-1.

The liner plate is predominantly 1/4-inch thick steel plate anchored to the containment structure concrete in the dome and

shell by 3 x 2 x 1/4-inch anchor angles with typical maximum spacings of about 15 inches. The horizontal liner plate in the base section is anchored to M 4 x 13 structural shapes embedded in the base concrete. The liner plate at the transition section (cone area shown in Figure 1) and at penetrations is heavier (typically ranging from 1/2 to 1 inch in thickness).

The dome was fabricated in sectors of about 10 feet with LCCs (channel bar sections 2 x 9/16 x 3/16-inches) covering the radial and circumferential butt joint segments joining the sectors. The LCCs project outward and are embedded in the containment structure dome concrete. The circumferential LCC segments run parallel to the anchor angle segments (see typical sections in Figure 5-2).

The shell liner plate was fabricated in typically 8 x 10-foot sections with similarly spaced anchor angles running vertically (see typical sections in Figure 5-3). Again, the 2-inch channel LCC sections were used to cover the circumferential and meridional liner plate butt joints. The shell LCCs project inward (to the inside of the containment) and do not directly interact with the containment structure shell concrete.

The base liner plate was fabricated in flat sections typically 10-feet wide by variable length (see Figure 5-4). Anchorage was achieved by welding to steel members (usually M 4 x 13 structural sections) embedded in the containment structure base mat concrete (see Figure 5-5) instead of the anchor angles as used in the shell and dome sections. Again, the 2-inch channel sections were welded over the adjoining butt joints to form inwardly projecting LCCs as shown in Figure 5-5.

Similar details were used in fabricating the pit area liner plate segments and LCCs except that embedded angles were used at exterior corners (instead of M 4 x 13 sections), 3 x 2 x 1/4-inch angles at about 15-inch spacing were used to anchor the



pit wall sections to the containment concrete similar to shell area and 1 x 1 x 3/16-inch angle sections were used to form LCCs at corners. The 1-inch angle sections were also used at the cone-to-base transition sections. All cone, base, and pit LCCs project inward.

Typical dome, shell, cone, base, pit, and penetration LCC details are shown in Figure 5-6.

The application and general location of these sections are as follows:

<u>Section</u>	<u>Application</u>	<u>Location</u>
1	1/4-inch liner plate butt weld	Shell and lower dome
2	Liner plate thickness transition butt weld	Shell - near penetrations
3	Electrical penetration (single or multiple)-to-thickened plate welds	Shell
4	Transition shell-to-cone liner plate butt weld	Near base
5	Cone section thickness and angle transition butt weld	Near base
6	Cone-to-base butt weld	At base
7	1/4-inch liner plate butt weld	Base
8	1/4-inch liner plate butt weld at base-to-pit outside corner	Base
9	1/4-inch liner plate butt weld at base-to-pit inside corner	Pit
10	Seal weld on equipment hatch	Shell
11	Pipe cone-anchor weld (main steam and feedwater pipes)	Shell
12	Same as Section 11 except at weld of anchor to thickened liner plate	Shell
13	Construction vent closure weld	Top of dome



The LCCs were typically fabricated from 2-inch channel, 1-inch angle, 1/4-inch plate, or 2-1/2-inch standard pipe sections and attached to the liner plate (or penetration) with a 3/16-inch double-pass fillet weld (in accordance with Specification C7, Reference 7). Further descriptions, member sizes, and cross references to design drawing details are contained in Table 5-1.

#### 5.2.1 Test Pipes and Tubing

The LCC system is divided into several subcompartments to enable testing of a limited number or length of LCCs at any one time. The LCC sections are fitted with 3/4-inch diameter test pipes to facilitate pressurizing the subcompartments. In the cylinder, cone, base, and pit areas, the test pipes are welded directly to the LCC (with 3/16-inch double-pass fillet welds) because the LCCs project inward. In the dome section where the LCCs project outward (into the concrete), the test pipes are welded to the liner plate (again with 3/16-inch double-pass fillet welds) in line with a 3/4-inch diameter hole extending through the liner plate and directly into the LCC (see Figure 5-2). The test pipe connections are typically about 1-inch long except for the base and pit area where they extend through the upper slab concrete (see Figure 5-5). Except for some of the dome LCCs, the LCCs are typically sealed by 1/2-inch pipe plugs screwed into the end of the test pipe. In the upper portion of the containment (above elevation 98'-0"), selected LCCs were connected to 3/8-inch Type 316 stainless steel tubing which is routed to valve manifolds at elevation 70'-0" (data on the test tubing system are from References 9 and 10). As a result of some indeterminate aspects associated with the tubing system, it was decided to disconnect the tubing from the test pipes and seal the test connection (like the remainder of the LCC system).

This effectively removes the tubing system from the LCC system. Therefore, the tubing system is given no further consideration in this report.

### 5.3 STRUCTURAL BEHAVIOR AND ANALYTICAL APPROACH

The analytical approach utilized to assess the structural performance of the various LCC sections depended on the manner in which the LCCs are loaded to produce the most severe load, stress, strain, or displacement condition on the LCC. An examination of the liner plate LCC system indicated that for analytical purposes each LCC section could be placed in one of two major categories. In the first category (typical of the dome sections) the LCC projects outward and interacts with the containment structure concrete when relative displacement occurs between the liner plate and the concrete. The second category involves all other LCC sections which project inward and do not directly interact with the concrete.

In the first category, the loading on the LCC is a rather complex function of interactions with other elements of the liner plate system as well as with the concrete. Analyses in this case involved computer solutions of mathematical models representing the interacting system of elements with parametric evaluations to account for materials properties variations.

In the second category, the loading can be defined more locally, involving the LCC section and only the elements to which it is directly attached. In this case, there is usually little or no in-plane relative displacement of the liner plate with respect to the concrete. The analyses is less complex involving solution of forced displacements of the LCC section due to induced strains in the attached members along with the effects of directly applied pressure loads (if present). Although this type of loading occurs in both the outward and inward projecting LCCs, it is found to be the controlling case for only the inward project LCCs. Conventional structural analysis techniques are utilized with evaluations based on lower bound (specified or actual) physical material properties (no parametric evaluations are required).

The behavior of specific liner plate sections in these two categories are discussed in more detail in the following subsections.

#### 5.3.1 Plate Curvature

Due to the applied loads and associated induced strains, the liner plate (particularly in the shell and dome sections) is in a state of biaxial membrane compression. When the liner plate curvature is outward, the plate is stabilized by compression or bearing against the concrete. In this case, the plate is symmetrically stressed in both the meridional and circumferential (or hoop) directions and little or no relative displacement occurs between the liner plate and the concrete. This condition is typical in the second analytical category discussed in Section 5.3.

If inward curvature develops in one or more of the panels (as shown in Figures 5-2 and 5-3 (Case B), membrane compression is partially relieved by the inward movement of the plate causing relative motion between the liner plate and the concrete (creating analytical Category 1 conditions). This relative motion causes engagement and loading of angle anchors and LCCs (if present) with the concrete to maintain force balance.

#### 5.3.2 Exterior LCCs (Dome Section)

The dome section only contains exterior (outwardly projecting) LCCs running in both the meridional and circumferential directions. The circumferentially oriented anchor angles preclude buckling in the circumferential direction. Inward curvature can occur in panels between anchors as shown in Figure 5-2.

If inward curvature is absent over a distance of several panels, the loading on the LCCs (both meridional and circumferential)



will approach that of the shell section for similar conditions. The compressive strain levels in the dome section are lower than that for the shell (particularly near the base). Therefore, this is not a controlling condition in the dome for LCC loading.

The controlling loading for the embedded dome LCCs occurs in the LCCs that run parallel to the 3 x 2 x 1/4-inch anchor angle segments when the inward curvature (a bent plate) occurs in the adjacent liner plate panel (as shown in Figure 5-2). This will provide local relief for part of the compressive load in the liner plate, and the sections on both sides of the bent plate will move toward the bent plate. This results in relative movement between the liner plate and the containment structure concrete, which imparts shear loads into embedded anchor angles and LCC sections, the sum of which must bring the system back into force balance.

The determination of the resulting loading on the anchor angles and LCCs requires analysis of a sufficiently large section of liner plate so that the loads on the anchor angles (or LCCs) farthest removed from the bent plate section approach zero and the plate stresses (or strains) approach that of the continuous outward curvature fully restrained condition. The 97-1/2-inch-long section shown in Figure 5-2 was selected for this analysis and satisfies the foregoing conditions.

The general approach for the dome section analyses included the following:

- a. Definition of loads in terms of induced strains in the liner plate system (see Section 6.0)
- b. Definition of the load-deformation characteristics of each liner plate element (including the LCCs) with respect to variations in material strength properties in both the linear and nonlinear response ranges

- c. Development of a mathematical model of the liner plate LCC system which, along with Item b, properly accounts for the interaction of all elements of the system
- d. Conducting a parametric analysis of the system covering a range of component element material strength and deformation properties utilizing computer solutions of the mathematical model

A description of these analyses and a summary of pertinent results are given in Section 7.0.

### 5.3.3 Interior LCCs

Interior projecting LCCs are found in all major areas of the containment structure liner plate as shown in Figure 5-6 and summarized in Table 5-1. The interior LCCs are subjected directly to accident pressure and temperature loads as well as forced displacements due to induced strains in supporting elements. The controlling loading condition for the LCC sections usually occurs when the strain in the element(s) to which they are attached is at a maximum.

Outward curvature conditions, as shown in Figure 5-3, Case A, will produce more severe loading on the LCC than inward curvature, Case B. In Case B, the liner plate strain (and consequently the load on the LCC) is relieved by the inward curvature (bent plate) panel.

The analyses of these sections involved determining the forced displacements (from support element strain levels) and other concurrent loads on the LCC sections (such as accident pressure) and solving for the internal forces, moments, and/or strain levels using conventional structural analysis techniques.



A description of these analyses and a summary of their results are contained in Section 8.0.

#### 5.4 MATERIALS PROPERTIES

##### 5.4.1 Liner Plate and LCC Components

The physical properties of the steel liner plate and LCC components are summarized in Table 5-2. In addition to ASTM-specified values, minimum, mean, and maximum values are also given for cases where physical properties variations are used in parametric analyses.

The maximum and minimum values for the 1/4-inch-thick liner plate represent the mean, plus or minus two standard deviations as determined from data contained in certified material test reports (CMTRs) furnished by the materials supplier.

Sufficient CMTRs were located to represent all of the 1/4-inch liner plate in both Unit 1 and 2 containments.

Although some CMTR data were available for the 2 x 9/16 x 3/16-inch channel bar stock LCC sections, the data represented an insufficient percentage of the total channel section population for reliable statistical inferences. Selection of the values shown in Table 5-2 is based on ASTM-specified values and typical observed values for other ASTM A 36 structural shapes. The 45 ksi mean value corresponds to available CMTR data. The 61.6 ksi maximum yield value corresponds to the yield strength of the LCCs used in the liner plate LCC tests discussed in Appendix B.

For all steel elements, Poisson's ratio was taken as 0.3 and the elastic modulus was taken as  $29 \times 10^6$  psi.

#### 5.4.2 Concrete

The physical properties of the concrete used in the analyses are summarized in Table 5-3. The maximum and minimum compression strength values used for the parametric analyses represent the mean plus or minus two standard deviations as determined from compression tests on the 90-day-old standard concrete cylinders sampled from the domes of each unit during concrete placement. The dome concrete data were utilized for this investigation because they would be more representative for investigating LCC-dome concrete interaction. The concrete strength data were sufficient to provide full coverage (based on volume comparisons) for both domes. The strength values for the shell concrete were comparable.

Poisson's ratio data were obtained from Reference 5. Poisson's ratio was assumed to be invariant with concrete compressive strength.

Elastic modulus data were also obtained from Reference 5. For the purposes of extending these data to other concrete strengths, the elastic modulus was assumed to be proportional to the square root of the concrete compressive strength.

TABLE 5-1 - LOCATION AND DESCRIPTION OF INTERNAL LCC SECTIONS

(1) Section	Location	Application	Reference Drawing	Reference Detail	Member Size	Notes
1	Shell	LP butt weld	C-123	1, 3, 4	[ 2 x 9/16 x 3/16	Typical detail at butt welds joining 1/4-inch liner plate sections - horizontal and vertical joints similar
2	Shell	Plate thickness transition	C-121 C-123 C-124	1 5 i-6,8,9	[ 2 x 9/16 x 3/16	Transition from 1/4 inch to a thicker liner plate such as at penetrations, brackets, etc
3	Shell	Electrical penetration	C-122 C-124	5,12	PL 1-1/2 x 1/4 PL 3-1/2 x 1/4 PL 1-1/4 x 3/8 PL 3-1/2 x 3/8	Can occur singularly or in multiple clusters on one thickened plate  Heavier plate at skewed penetration in shell-to-base cone transition
4	Shell	LP butt weld	C-123	3	[ 2 x 9/16 x 3/16	Cylinder-to-cone transition, 1/4-inch liner plate
5	Shell	LP butt weld	C-123 C-126	3 Sect. D	L 1 x 1 x 3/16	Transition 1/4-inch LP cone to 1/2-inch LP cone near base; LCC protected by expansion joint and 1/2-inch styrofoam
6	Base	LP butt weld	C-123	3	L 1 x 1 x 3/16	Transition 1/2-inch LP cone LP to 1/4-inch base LP; covered with 1'-6" of concrete and protected with 1/2-inch styrofoam (see Figure 5-6)
7	Base	LP butt weld	C-126 C-130	1, 2 2	[ 2 x 9/16 x 3/16	Typical LCC in flat base section (see Figures 5-5 and 5-6)
8	Base (pit)	LP corner butt weld	C-126	5	L 1 x 1 x 3/16	Outside corner detail - embedded in concrete and protected with 1/2-inch styrofoam
9	Base (pit)	LP corner butt weld	C-126	4	1 x 1 x 3/16	Inside corner detail - embedded in concrete and protected with 1/2-inch styrofoam
10	Shell	Hatch cover	C-121		2-1/2-inch diameter <sup>(2)</sup> steel pipe sector	LCC for closure weld on equipment hatch and lock plate
11	Shell	Main steam and feed-water pipes	C-124	2	2-1/2-inch diameter <sup>(2)</sup> steel pipe sector	At butt weld in 1-inch anchor cone
12	Shell	Main steam and feed-water pipes	C-124	2	PL 2" x 1/4" <sup>(2)</sup> PL 3" x 1/4"	At 1-inch cone to thickened plate butt weld
13	Dome	Closure plate	C-123	9, 10	[ 2 x 9/16 x 3/16	Closure plate for 12-inch construction vent in dome

Notes:

(1) For configuration see Figure 5-6.

(2) Approximate; size not specified on drawing.

TABLE 5-2 - LINER PLATE AND LCC ELEMENT PHYSICAL PROPERTIES

Component	ASTM	Grade	Range	Strength Properties		
				Yield (ksi)	Ultimate (ksi)	Elongation <sup>(1)</sup> (%)
Liner plate (1/4-inch thick)	A 442	60	Min	45	60	
			Mean	50	65	
			Max	55	70	
			ASTM	32	60-80	20
Liner plate (1/2 to 1-inch thick)	A 516	60	ASTM	32	60-80	21
	A 516	70		38	70-90	17
LCC sections 2 x 9/16 x 3/16 channel	A 36		Min	36	58	
			Mean	45	70	
			Max	61.6	80	
			ASTM	36	58-80	20
LCC section 1 x 1 x 3/16	A 36		ASTM	36	58-80	20
LCC section 1/4-inch plate	A 36		ASTM	36	58-80	20
	A 442	60	ASTM	32	60-80	20
	A 516	60	ASTM	32	60-80	21
	A 516	70	ASTM	38	70-90	17
Anchor angle 3 x 2 x 1/4	A 36		ASTM	36	58-80	20
Pipe	A 53	A	ASTM	30	48	>20
	A 333	1	ASTM	30	55	28
	A 333	6	ASTM	35	60	24
LCC weld filler material	A 233 <sup>(2)</sup>			50-60	62-72	22
	A 559 <sup>(3)</sup>			60	72	22

(1) Percent elongation values given are for 8-inch gage length test specimens except for ASTM A 53, Grade A, pipe and weld material which are for 2-inch gage length specimens.

(2) Designation discontinued, compares to current AWS Specifications E 60XX and E 70XX.

(3) Designation discontinued, compares to current AWS Specification ER 70S-X.



TABLE 5-3 - CONCRETE PHYSICAL PROPERTIES

<u>Compression Strength</u> (ksi)		<u>Elastic Modulus</u> (ksi)	<u>Poisson's</u> <u>Ratio</u>
Minimum	6	$4.3 \times 10^3$	0.24
Mean	8.5	$6.8 \times 10^3$	0.24
Maximum	11.0	$7.74 \times 10^3$	0.24
Minimum Specified	5.0	-	-

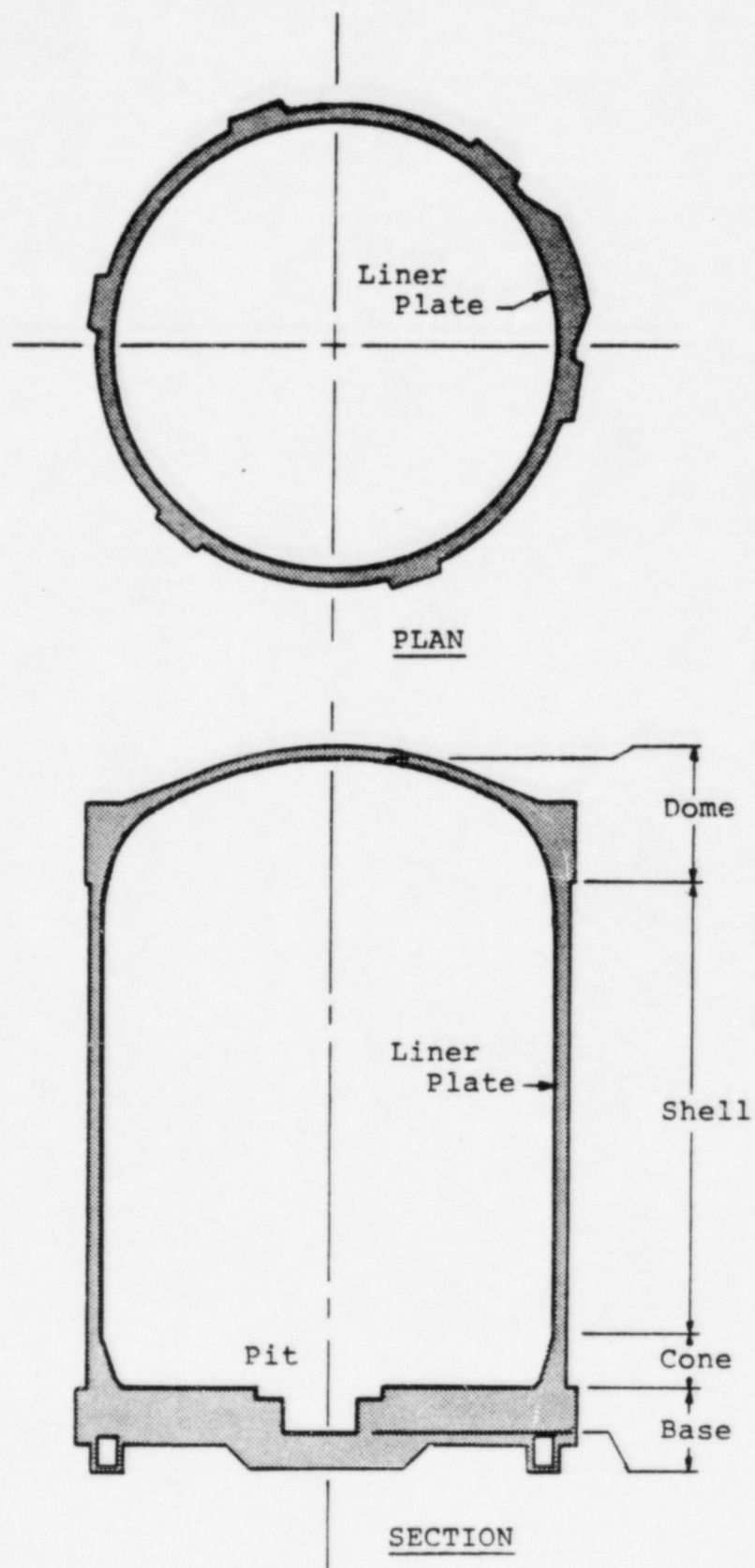


Figure 5-1 Liner Plate Locations

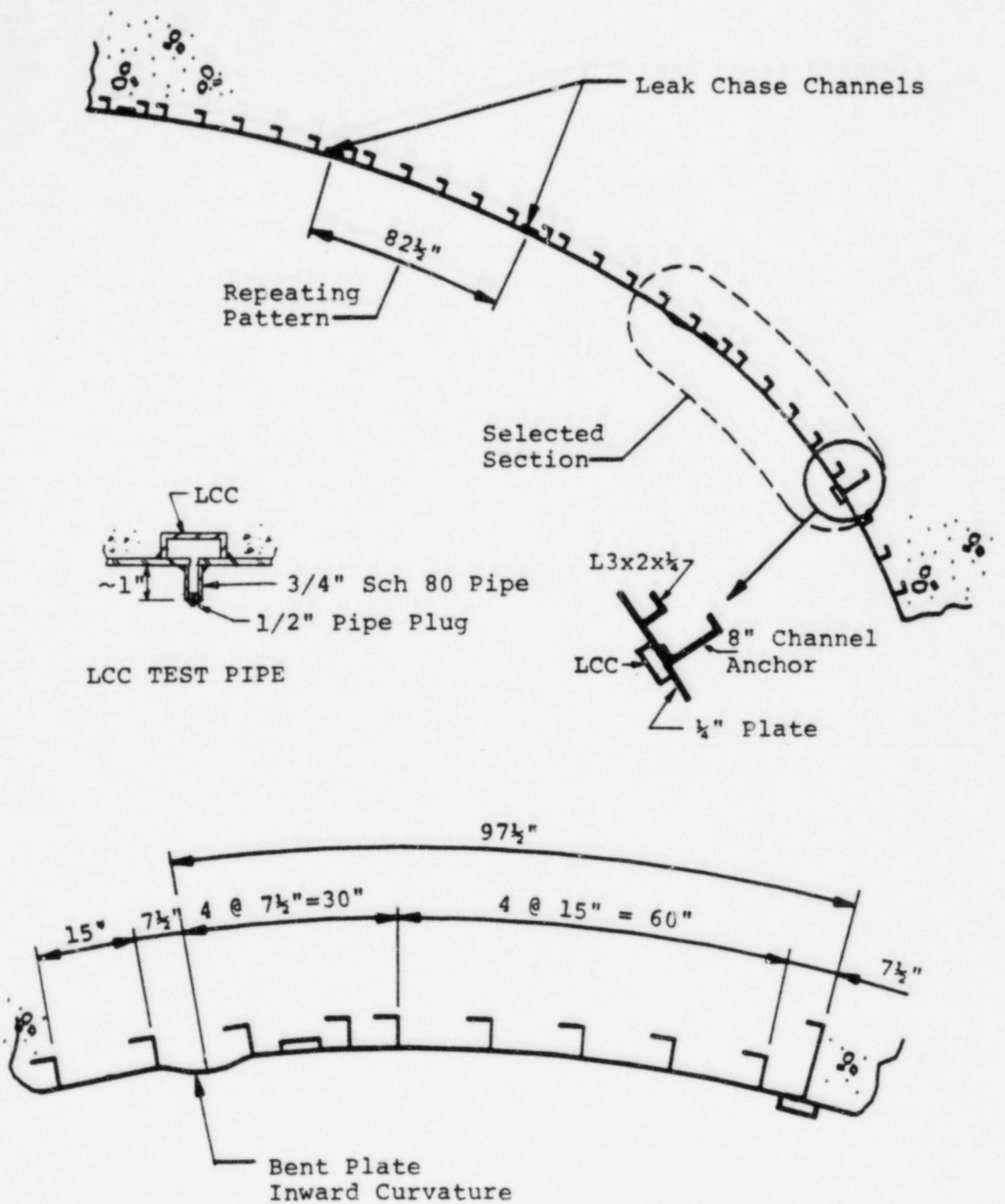


Figure 5-2 Dome Liner Plate Section and Details

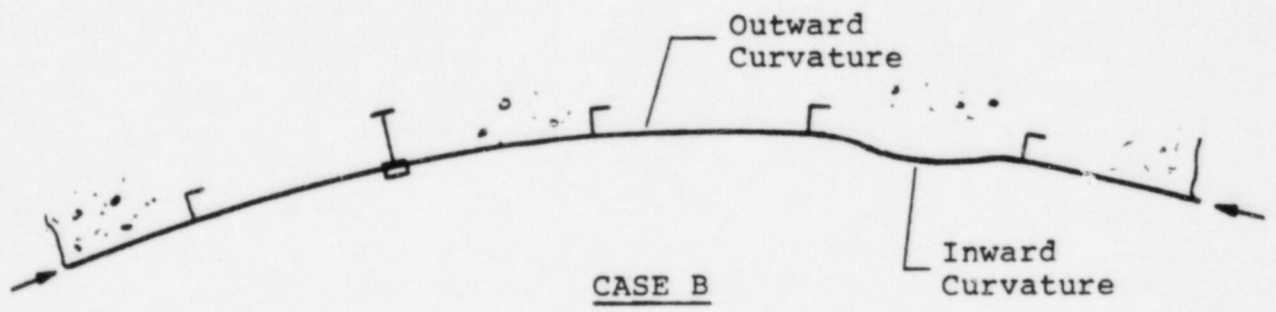
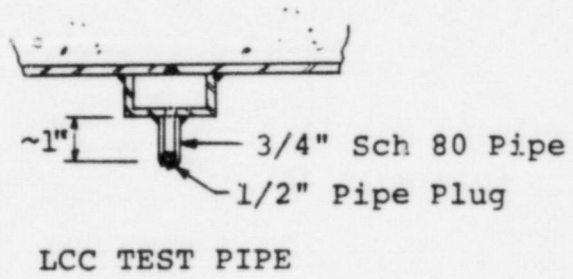
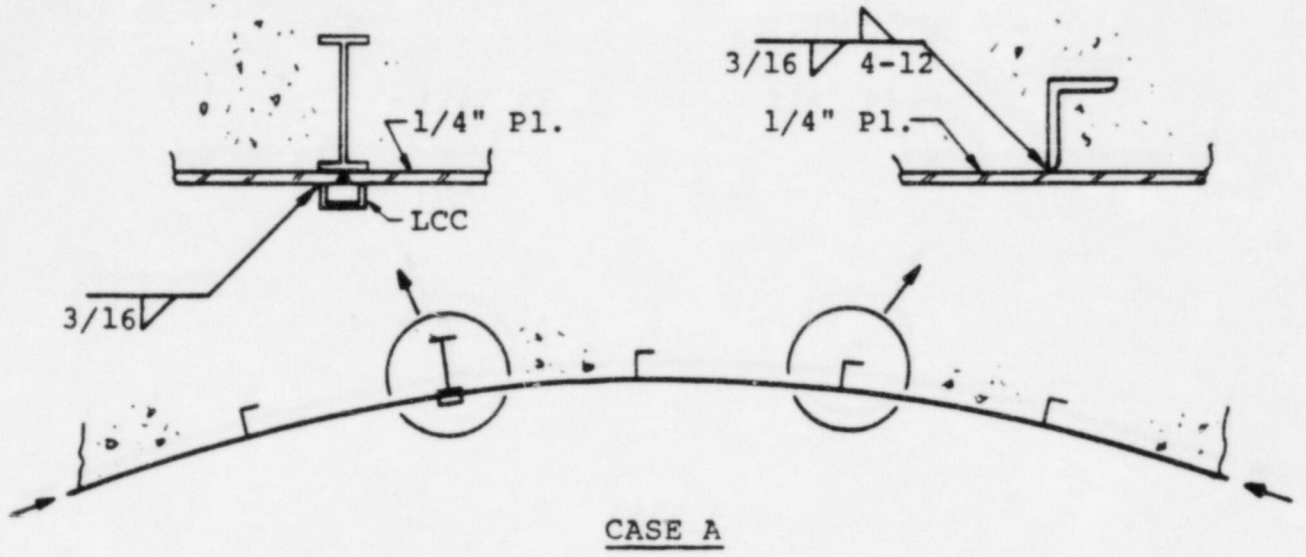


Figure 5-3 Typical Cylindrical Shell Sections



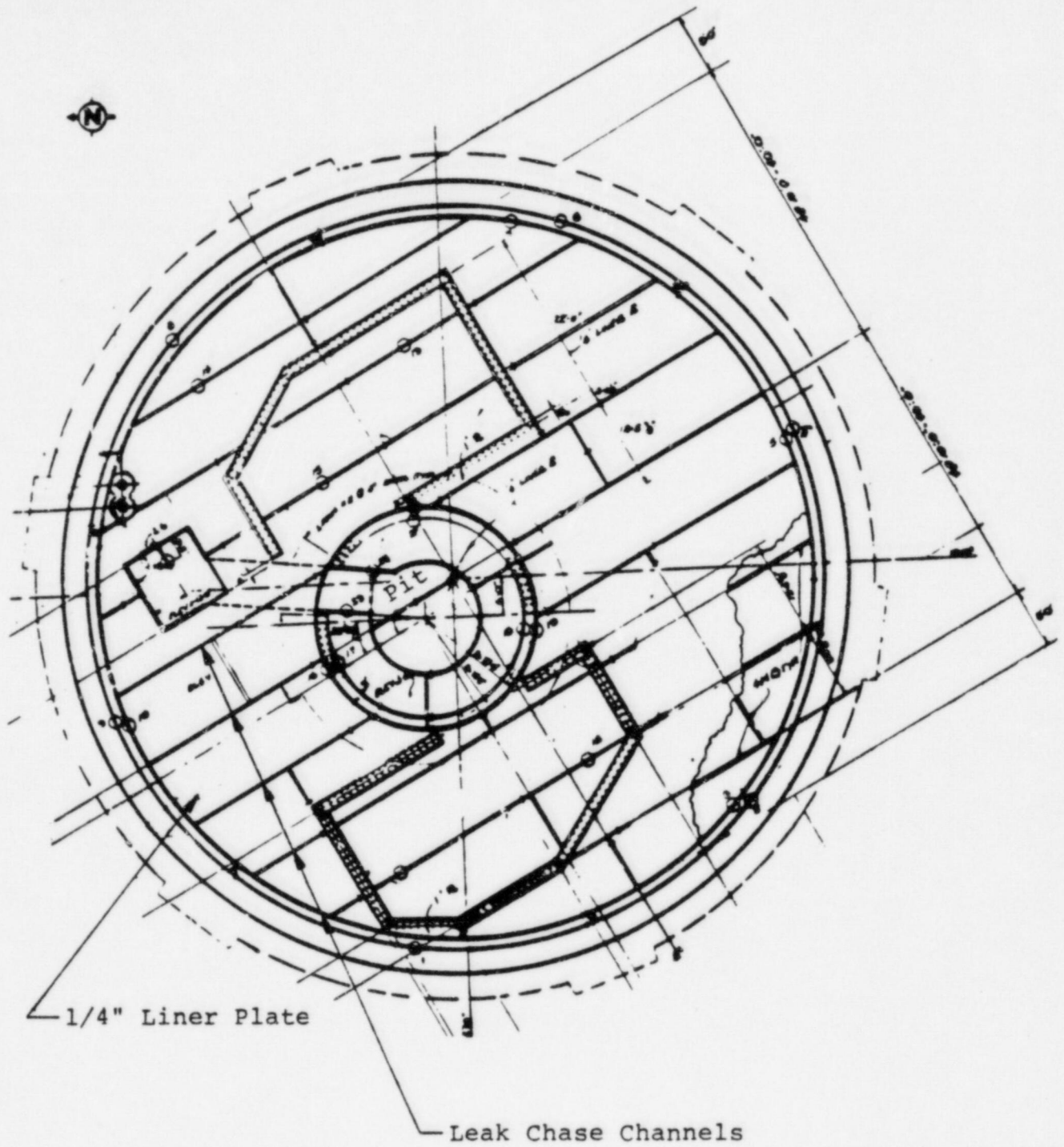


Figure 5-4 Leak Chase Channel and Seal Weld Location in Base Liner Plate

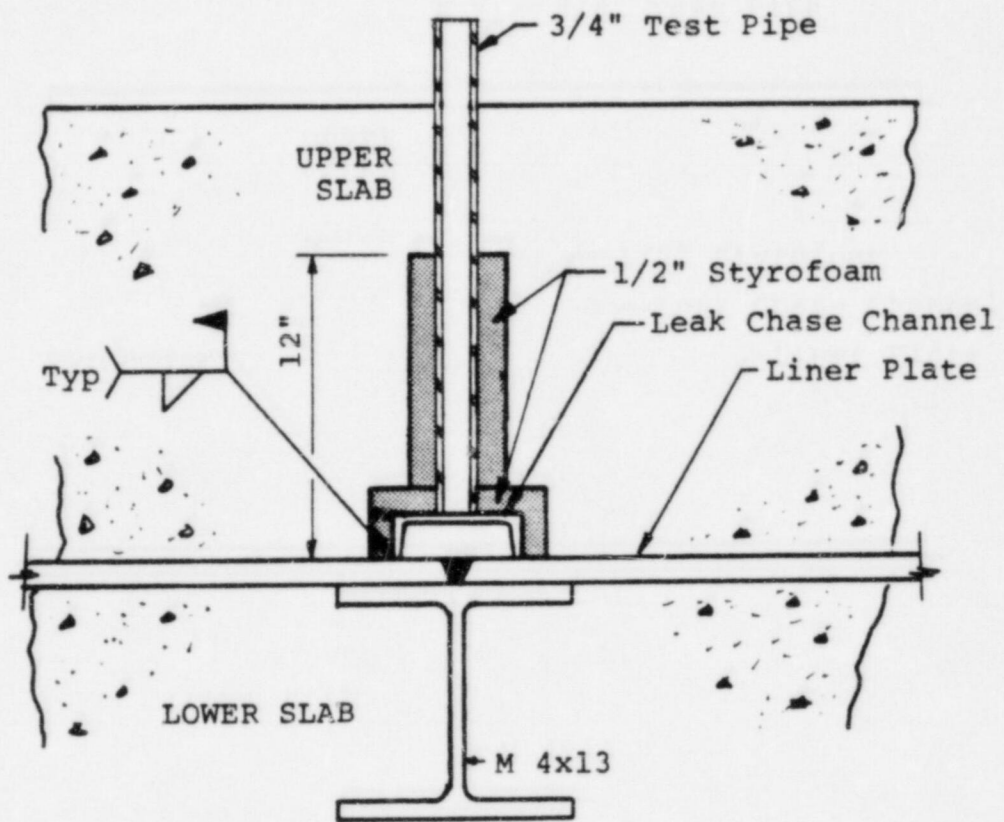


Figure 5-5 Typical Leak Chase Channel Detail in Base Slab

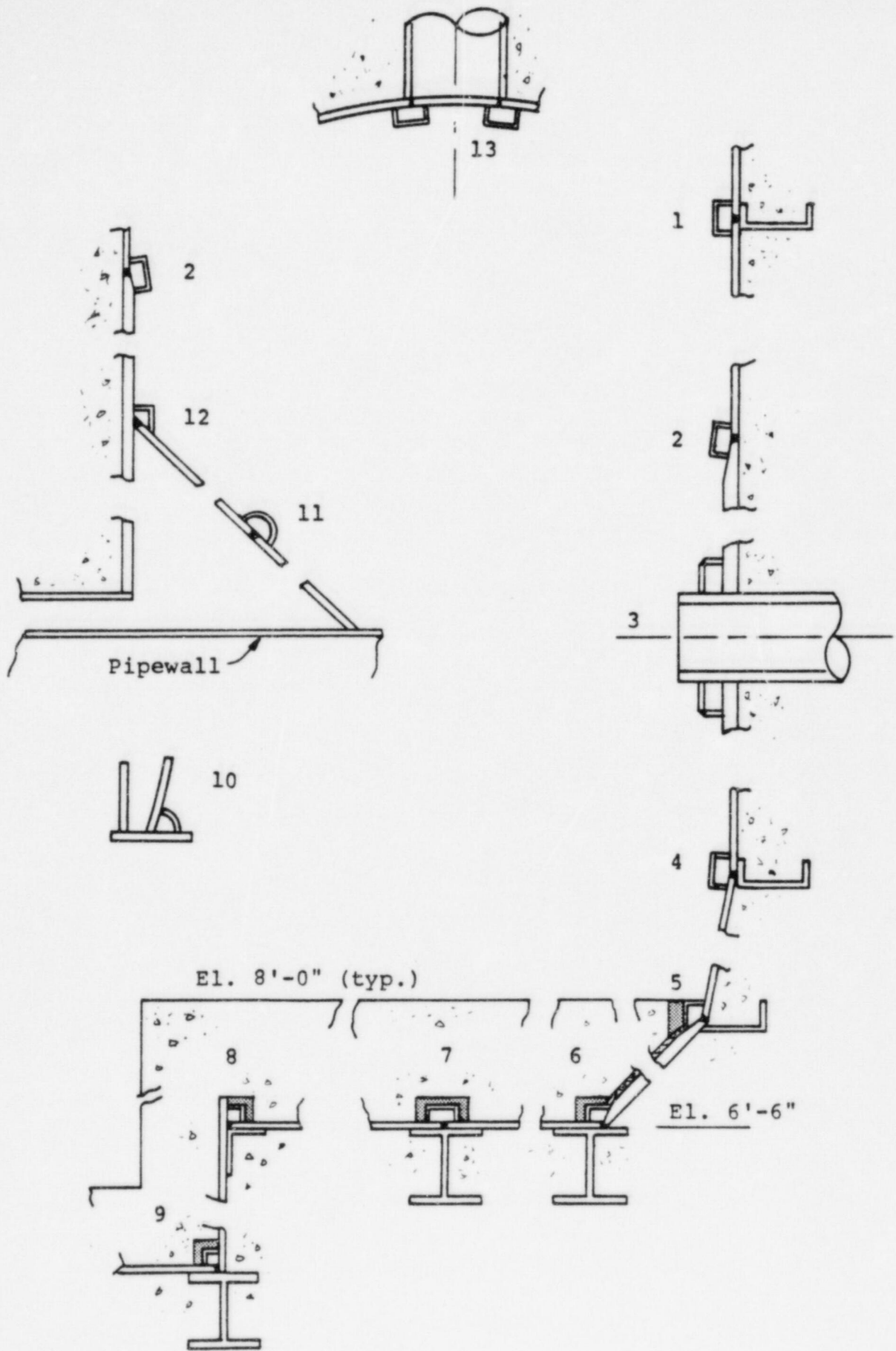


Figure 5-6 Typical Interior LCC Sections

## 6.0 LOADS

The loads utilized in this investigation were derived from those contained in the plant FSAR (Reference 1). Because the loads in the liner plate LCC system are predominantly a direct function of the relative strain between the liner plate and the containment structure concrete, the loads from the FSAR were redefined in terms of relative strain. The resulting relative strains for the dome and shell sections for various loading conditions are summarized in Table 6-1. For convenience in presenting small numbers, the relative strain values are given in units of microstrain,  $\mu$  ( $1\mu = 10^{-6}$  in./in.). For the sign convention used in Table 6-1, plus (+) indicates tensile strain and minus (-) indicates compressive strain.

The strains associated with the controlling load combination are also given in Table 6-1. The load combination is defined in terms of a load equation using the notation given for each loading condition. For convenient reference, a summary of notation used throughout this report is also contained in Appendix A.

In cases where strains were not given directly in Reference 1, conventional structural analysis techniques utilizing conservative assumptions such as the following were used to convert loads to strains:

- a. Calculation of concrete deformations were based on a lower limit elastic modulus of  $4.3 \times 10^3$  ksi which results in upper limit concrete strains.
- b. The temperature of the liner plate was assumed to be equal to the internal containment temperature. No thermal gradient across the plate was considered.



- c. An average concrete temperature (before accident,  $T_c$ ) of 60F was assumed in determining average differential temperatures.

Only one value of strain is given for the dome hoop and meridional directions since these strains in this area are nearly equal. Differences in hoop and meridional strains in the shell sections are due to the asymmetry associated with prestress, pressure, seismic, and dead loads.

The liner plate in the base and pit sections is subjected to a low-level thermal strain due to the comparatively low slope of the thermal gradient through the base slab, liner plate, and upper concrete cover section (for top slab and protective wall sections - see Figures 5-5 and 5-6). The maximum base liner plate strains would be on the same order as the maximum estimated base slab concrete and reinforcing steel strain (about 830  $\mu$ , from concrete and steel stress limits).

To demonstrate the adequacy of the clearance provided by the styrofoam around the LCCs and their test pipes, the following, very conservative assumptions were made:

- a. The thermal gradient in the upper concrete cover was not considered and the concrete temperature was assumed to be equal to the postulated internal accident temperature (286F).
- b. The liner plate temperature was assumed to remain constant at an average temperature (existing just prior to the postulated accident) of 55F.

This resulted in a strain level of 1,500  $\mu$  corresponding to an effective differential temperature of 231F.

The 1/2-inch minimum thickness styrofoam spacer protection was shown to be adequate (see Section 8.5), therefore, further refinements were not required.

TABLE 6-1 - LOAD SUMMARY IN TERMS OF RELATIVE STRAIN

Notation	Description	Relative Strain ( $\mu$ ) <sup>(1)</sup>		
		Dome <sup>(4)</sup>	Shell Meridional	Shell Hoop
D	Dead load - (Near base of shell)	(2)	-38	+9
$\Delta P$	Differential pressure (2 psi)	$\pm 5$	$\pm 2$	$\pm 6$
$P_a$	Accident pressure (60 psi)	+138	+51	+185
$E'$	Seismic (DBE-near shell base)	(2)	$\pm 30$	$\pm 17$
$P_s$	Prestress	-207	-61	-273
S	Shrinkage	-103	-103	-103
C	Creep	-190	-97	-190
$T_o$	Operating thermal (Avg $\Delta T = 50^\circ F$ )	-325	-325	-325
$T_a$	Accident thermal ( $T_{max} = 286^\circ F$ , $T_c = 60^\circ F$ )	-1470	-1470	-1470
$U^{(3)}$	$D + P_s + S + C + P_a + T_a + E'$	-1832	-1748	-1859

(1) Strains given in microstrain,  $\mu$ , units  $1\mu = 10^{-6}$  in./in.

(2) Very small strain level ignored in analyses

(3) Controlling load combination

(4) Values given are for both hoop and meridional directions

## 7.0 EMBEDDED LCC SECTION ANALYSIS

### 7.1 SECTION SELECTION

Liner plate LCC sections embedded in and in direct contact with the containment structure concrete occur only in the dome area (bounded by the 8-inch circumferential anchor channel shown in Figure 5-2). A general description of the dome liner plate and LCCs is given in Section 5.0.

The most severe shear loading occurs on the LCCs which run parallel to the circumferential anchor angles. These anchor angles preclude circumferential buckling and transfer stresses between the liner plate and the concrete due to any unbalanced circumferential strains. Therefore, embedded radial LCCs would be subjected to minimal transverse shear and large axial compression loads from the liner plate similar to the LCCs in the shell section. The compressive strain level in the dome is slightly less than that in the shell hoop direction. Therefore, this was not considered a potentially controlling stress or deformation condition (or section location) in the dome. The more severe shell condition is treated in Section 8.0.

The more severe loading conditions in the dome would result from relief of meridional strains due to inward curvature of a 15-inch-wide liner plate panel (bent plate) adjacent to a circumferentially oriented LCC.

The section considered the most severely loaded was near the outer perimeter of the dome where the circumferential LCCs change from projecting inward (into the containment) to projecting outward into the dome concrete. An enlarged view of this section is shown in Figure 5-2. The 8-inch channel section (embedded into the concrete) is welded to the liner plate opposite the last inward-projecting LCC section. This functions



as a substantial anchor which is assumed to be rigid in the analysis.

The partial relief of liner plate membrane stresses in the bent plate panel causes the liner plate from the 8-inch channel to the bent plate panel to move toward the dome apex along the concrete surface (meridionally) causing shear forces on all angle anchors and on the LCC in the panel adjacent to the bent plate panel section. The other similar inner liner plate section (repeating pattern show in Figure 5-2) would concurrently move outward toward the cylindrical shell. The LCC in this second section would be much less severely loaded because it is located in a panel with five angle anchors between it and the inwardly curved panel. Therefore, only the outer section was analyzed. For analytical purposes the meridional displacement of the inwardly curved panel is assumed to be equally shared by the inner and outer liner plate sections (displacement of the bent plate panel is assumed to be symmetrical about its midpoint). This results in essentially zero meridional displacement at the midspan of the inwardly curved panel.

The resulting 8-foot, 1-1/2-inch-long section is sufficiently long to allow equalization of liner plate stresses at liner plate elements approaching the anchor channel end of the section (see Elements 6 through 10 in Table 7-3).

## 7.2 MATHEMATICAL MODEL

The selected section was idealized as a one-dimensional system of springs in the mathematical model shown schematically in Figure 7-1.

The center of the bent plate section is treated as an anchor at Node 2. The 8-inch channel section is represented as an anchor at Node 11. Interaction of the LCC with the concrete at Node 1 is modeled by appropriate selection of the spring properties of the LCC (Element 1). Similar interaction of the angle anchors,

Elements 11 through 17, with the concrete at Nodes 12 through 16, is modeled by appropriate selection of angle anchor spring properties. The spring properties of these two elements (LCC and AA) include both the steel deformation in the element and the deformation of the engaged concrete. The spring properties of the remaining bent plate short plate, and long plate elements are controlled by the physical properties of the liner plate steel.

For modeling purposes, a 1-inch-wide meridional strip of liner plate is used (plate, anchor anchors, and LCCs). Although one-dimensional representations of the bilinear spring elements is used, two-dimensional strain conditions are accounted for in defining the spring properties of the liner plate elements.

The physical properties of the liner plate spring elements used in the parametric analyses discussed in Sections 7.4 and 7.5 are summarized in Table 7-1.

The low, mean, and high (L, M, and H) values given in Table 7-1 reflect the corresponding minimum, mean, and maximum steel and concrete strength properties contained in Tables 5-2 and 5-3. For bases for these variations see Section 5.4.

The bilinear characteristics of these springs is shown schematically in Figure 7-2 along with the definition of spring element terms used in Table 7-1 and elsewhere in this report.

The properties of the bent plate, short plate, long plate, and anchor angle elements are based on the test data and procedures contained in Reference 4. The short and long plate elements are similar, but differ only in length (7-1/2 and 15 inches, respectively).

The plastic range stiffness values for the short and long plate elements are based on the difference between the steel ultimate and yield strengths ( $f_u$  and  $f_y$ ) and a deformation at

ultimate load corresponding to a strain level of 10% (one-half of the minimum ASTM specified percent elongation (see Table 5-2)).

The properties of the LCC elements were developed from the test data in Reference 8 using procedures similar to those contained in Reference 4. The tests reported in Reference 8 were conducted in support of this investigation. A description of these tests and a summary of the development of LCC element strength properties for varying concrete and steel strengths are summarized in Appendix B.

### 7.3 MODEL SOLUTION

The mathematical model representing a system of bilinear springs was solved using a linear structural analysis computer program and the following reiterative procedure to account for nonlinearity.

- a. The system was loaded by introducing a forced displacement in the 1/4-inch liner plate elements (members 2 through 10 in Figure 7-1) corresponding to a uniform strain level until a force of  $R_y$  is reached in one of the elements (see Figure 7-2 for definition of terms). This was accomplished by subjecting the plate elements to an equivalent thermal load (a uniform differential temperature).
- b. For positive plastic stiffness ( $K_b$ ) springs, the elastic stiffness,  $K_a$ , was replaced with the plastic spring rate,  $K_b$ , and the force,  $R_o$ , applied at the appropriate node(s) (see Figure 7-2 for definition of terms).

For negative  $K_b$  springs (bent plate),  $K_a$  was replaced with  $K_b$ , set to a value approaching zero, and a force of estimated value  $R_m$  (bent plate



resisting force at maximum response to applied load) was applied to Node 3 in Figure 7-1. For the first iteration,  $R_m$  was set equal to  $R_y$ . The estimated value of  $R_m$  was readjusted with respect to displacement until an acceptable agreement was reached between calculated and estimated values of  $R_m$ .

- c. The process was reiterated for next springs to reach  $R_y$  until the thermally induced strain matched the relative strain between the steel liner plate and the concrete with all elements responding in the proper mode (elastic or plastic) depending on their calculated displacements.

#### 7.4 LOAD CASES

The load and displacement induced into the LCC sections (due to relative displacement between the liner plate and the concrete) is not only a function of the magnitude of the relative displacement, but also a function of the bilinear strength and stiffness properties of the LCCs with respect to those of the other liner plate spring elements.

The set of load cases summarized in Table 7-2 considering variations of strength and stiffness values of the various elements was therefore devised to isolate the controlling combination of spring element values that would result in the maximum loading conditions on the LCC sections. From a study of the structural behavior of the system, it was deduced that a LCC with low stiffness would attract higher displacements in combination with strong, stiff, straight plate elements (maximum strength range) and lower strength and less stiff bent plate and anchor angle elements. This resulted in the combination of spring element properties for Load Case 1. By similar logic, higher LCC loads would be produced by a high LCC stiffness with



the same combination of other element spring properties (Load Case 2).

Load Cases 3, 4, and 5 were included to illustrate the effect of variation of strength properties using all low, medium, or high (L, M, or H) values for all elements.

Load Case 6 was devised to illustrate the effect of adding (or deleting) the LCC section from the system. The effect of removing the LCC can be determined by comparing Load Case 6 (with LCC removed) with Load Cases 1 and 2 which used identical properties for other elements.

Load Case 7 is included to evaluate the effect of induced axial loads on the bent plate plus frictional loads on the remaining liner plate elements due to the accident pressure (60 psig).

An input differential temperature of 282F corresponding to a liner plate-to-concrete differential strain level of 1832  $\mu$  (from Table 6-1) was used for all load cases.

An axial compression force of 1370 pounds was applied at Node 3 in Case 7 to account for the induced axial force on the bent plate due to the 60 psig accident pressure (load defined using Reference 4 procedures). Axial forces of 135 pounds each were applied at Nodes 3, 4, and 5 to account for frictional effects of the 60 psig accident pressure load on short plate Elements 3, 4, and 5. An axial force of 270 pounds was applied at Node 6 to account for the frictional force associated with accident pressure on long plate Element 6. The 60 psig accident pressure produced no additional frictional forces on the remaining plate elements (7 through 10) since the unbalanced forces on these elements were insufficient to mobilize the friction forces.

In determining the frictional forces, a lower limit coefficient of friction value of 0.3 was used.

## 7.5 RESULTS OF ANALYSES

The resulting element loads and displacements for Load Cases 1 through 7 are summarized in Table 7-3. The response mode for each element in each load case is given in Table 7-2, along with element strength range identification. The response is either elastic or plastic as indicated by E or P in Table 7-2.

The following considerations led to the selection of Elements 1, 2, 3, 9, 10, and 11 as key elements for purposes of comparison of load cases. Element 1 (the LCC) is, of course, the primary interest. Element 2 (the bent plate) is one-of-a-kind and has a significant effect on the LCC loading. Element 3 (short plate) can be of different material than the remaining plate elements (due to different plate sections being joined at the LCC location at Node 4). Long plate Element 9 and short plate Element 10 were consistently the highest stressed elements of these two groups. Anchor angle Element 11 was, likewise, the highest stressed element of the anchor angle group.

A summary of liner plate element properties ( $R_o$ ,  $R_y$ ,  $R_u$ ,  $X_y$ , and  $X_u$ ) strength range (L, M, or H) maximum response load ( $R_m$ ) and displacement ( $X_m$ ) value and response mode (E or P) are given in Tables 7-4 through 7-10 for Load Cases 1 through 7. (See Figure 7-2 and Table 7-2 for definition of terms.)

For comparison purposes, the calculated element response is also given in terms of load ratios ( $R_m/R_u$ ), displacement ratios ( $X_m/X_y$ ), and energy ratios,  $SF_e (U_u/U_m)$ .

$R_m$  = Response load on element (k/in.)

$R_u$  = Ultimate load capacity of element (k/in.)

$X_y$  = Yield displacement of element (in.)

$X_m$  = Response displacement of element (in.)

$X_u$  = Ultimate displacement of element (in.)

$U_m$  = Response ductility ratio

$$U_m = \frac{X_m}{X_y}$$

$U_u$  = Ultimate ductility ratio

$$U_u = \frac{X_u}{X_y}$$

$SF_e$  = Safety factor based on strain energy (or strain energy ratio)

$$SF_e = \frac{E_u}{E_m}$$

$E_u$  = Strain energy at ultimate load and displacement - or total area under load vs. displacement curve (in.-kips)

$E_m$  = Strain energy at maximum response - or area under load vs. displacement curve to displacement  $X_m$  (in.-kips)

The load ratios  $R_m/R_u$  demonstrate reserve load or resistance capacity. Displacement ratios  $X_m/X_u$  and  $U_m$  demonstrate reserve displacement capacity. Comparing ductility ratios  $U_m$  with  $U_u$  would give the same results as comparing displacements  $X_y$  and  $X_u$ .

The safety factor based on strain energy,  $SF_e$ , as used in the plant FSAR (Reference 1) reflects both reserve load and displacement capacity. Although the acceptance criteria contained in Reference 1 are subjective (without definite numerical values), acceptable values of  $SF_e$  should be greater than 2.

For comparable comparisons, the following guidelines can be used:

$$\frac{R_m}{R_u} < 1.0 \text{ for } K_b > 0$$



$$\frac{R_m}{R_u} > 1.0 \text{ for } K_b < 0$$

$$X_m > X_y$$

$$\frac{X_m}{X_u} < 0.5$$

$$\frac{U_m}{U_u} < 0.5$$

An examination of Tables 7-4 through 7-10 shows that all of the foregoing criteria are satisfied by all of the most severely loaded elements (of their type) for all seven load cases.

Comparisons of capacity and response values for the LCC (Element 1) only are shown in Table 7-11 for all load cases (except for Case 6 where the LCC was deleted). This table shows that Case 1 is the most severe loading condition with respect to the LCC. Although  $R_m$  values for Cases 2, 4, and 5 exceed that for Case 1,  $R_m/R_u$  value for Case 1 (0.499) is higher and  $SF_e$  value (11.3) is lower than for all other cases. For LCC steel deformation, Case 2 controls (see Section 9.0).

When the bent plate reaction is increased and frictional effects associated with the accident pressure are accounted for, the safety factor,  $SF_e$ , increases to 16.6 (Case 7). Load Case 7 is essentially Load Case 1 with added accident pressure effects.

The beneficial effect of the presence of the LCC can be seen by comparing Load Case 6 (LCC deleted) with Load Case 1. Load Case 6 is the same as Load Cases 1 and 2 with the LCC deleted. The bent plate (Element 2) safety factor drops from 3.4 to 2.6 and the anchor angle (Element 11) safety factor drops from 10.8 to 6.6 while the lowest plate (Element 9) safety factor increases from 118 to 122. The increase in this large safety factor is insignificant compared to the decrease in safety factor for the more critical anchor angle. The anchor angle is



more critical than the bent plate since it could fail at a much lower displacement than for the bent plate. A safety factor of unity for the bent plate would only indicate the mathematical limit for the idealized spring model, not incipient failure. The bent plate, in actuality, may be impossible to fail (lose continuity) in this mode.

The effect of uniformly low, medium, or high (L, M, or H) element strength properties can be seen by comparing Load Cases 3, 4, and 5. These cases indicate that as strength and stiffness of all elements are increased, the LCC safety factor  $SF_e$  increases (16.2 to 56.6), along with load capacity and displacement margins (see Table 7-11).

A comparison of Tables 7-6, 7-7, and 7-8 indicates similar increases for Elements 2, 9, 10, and 11 (bent plate, long plate, short plate, and anchor angle). Short plate Element 3 indicates a slight decrease in safety factor  $SF_e$  from 426 to 410 which is insignificant for this range of  $SF_e$ .

The overall LCC performance in the liner plate system is summarized as follows:

- a. The lowest calculated safety factor,  $SF_e$ , of 11.3 (Case 1) is well above a lower bound acceptable value of about 2.
- b. The calculated safety factor is increased to 16.6 when accident pressure (of 60 psig) is considered acting on the plate (Case 7 vs. Case 1). The presence of internal positive pressure increases LCC safety margins.
- c. The presence of the LCC increases safety margins for other critical elements of the liner plate system. For example, the safety factor,  $SF_e$ , for the anchor angle increased from 6.6 for Case 6 with no LCC, to 10.8 for

Case 1 with the LCC in place (all other factors being equal in the two cases).

Both tests and analysis have shown that the embedded LCCs are rugged components and well suited to function as an integral part of the dome liner plate system. Their structural benefits improve the overall safety margins of the system.

For a discussion of leaktight integrity with respect to predicted displacements, see Section 9.0.

TABLE 7-1 Spring Element Properties

Component	Element ID (1)	Strength Property (2)	Strength Property Value (3)		
			Low (L)	Mean (M)	High (H)
Leak Chase Channel (LCC)	1	Ro (k)	2.124	2.528	2.876
		Ry (k)	2.261	2.716	3.113
		Ru (k)	5.226	7.31	9.582
		Xy (in)	0.00398	0.00462	0.00518
		Xu (in)	0.09001	0.11750	0.14612
		Ka (k/in)	567.6	587.5	600.9
		Kb (k/in)	34.47	40.66	45.90
Bent Plate (BP)	2	Ro (k)	3.40	3.78	4.16
		Ry (k)	2.97	3.30	3.63
		Ru (k)	1.15	1.52	1.90
		Xy (in)	0.02286	0.02540	0.02794
		Xu (in)	0.120	0.120	0.120
		Ka (k/in)	130.0	130.0	130.0
		Kb (k/in)	-18.80	-18.80	-18.80
Short Plate (SP)	3.4 5.10	Ro (k)	11.20	12.44	13.69
		Ry (k)	11.25	12.5	13.75
		Ru (k)	15	16.25	17.5
		Xy (in)	0.01059	0.01177	0.01294
		Xu (in)	0.761	0.762	0.763
		Ka (k/in)	1062	1062	1062
		Kb (k/in)	5.00	5.00	5.00
Long Plate (LP)	6.7 8.9	Ro (k)	11.20	12.44	13.69
		Ry (k)	11.25	12.5	13.75
		Ru (k)	15	16.25	17.5
		Xy (in)	0.02118	0.02353	0.02589
		Xu (in)	1.521	1.524	1.526
		Ka (k/in)	531	531	531
		Kb (k/in)	2.50	2.50	2.50
Anchor Angle (AA)	11.12 13.14 15.16 17	Ro (k)	4.054	4.113	4.125
		Ry (k)	4.2	4.2	4.2
		Ru (k)	5.0	5.0	5.0
		Xy (in)	0.01932	0.01222	0.01073
		Xu (in)	0.125	0.125	0.125
		Ka (k/in)	217.4	343.8	391.3
		Kb (k/in)	7.57	7.09	7.00

(1) for element location see Figure 7-1

(2) for definition of terms see Figure 7-2

(3) Low, Mean, and High correspond to minimum, mean and maximum material strength values given in Tables 5-2 and 5-3

TABLE 7-2 Parametric Evaluation Matrix

Case No.	Element (1) ID No. (2)	LCC 1	BP 2	SP 3	SP 4	SP 5	LP 6	LP 7	LP 8	LP 9	SP 10	AA 11	AA 12	AA 13	AA 14	AA 15	AA 16	AA 17
1	Material (3) Response (4)	L P	L P	L E	H E	H E	H E	H P	H P	H P	H P	L P	L E	L E	L E	L E	L E	L E
2	Material (3) Response (4)	H P	L P	L E	H E	H E	H E	H P	H P	H P	H P	L E	L E	L E	L E	L E	L E	L E
3	Material (3) Response (4)	L P	L P	L E	L E	L E	L P	L P	L P	L P	L P	L E	L E	L E	L E	L E	L E	L E
4	Material (3) Response (4)	M P	M P	M E	M E	M E	M P	M P	M P	M P	M P	M P	M E	M E	M E	M E	M E	M E
5	Material (3) Response (4)	H P	H P	H E	H E	H E	H P	H P	H P	H P	H P	H P	H E	H E	H E	H E	H E	H E
6	Material (3) Response (4)	(5) (5)	L P	L E	H E	H E	H E	H E	H E	H E	H P	L P	L E	L E	L E	L E	L E	L E
7	Material (3) Response (4)	L P	L P	L E	H E	H E	H E	H E	H P	H P	H P	L E	L E	L E	L E	L E	L E	L E

(1) LCC = Leak Chase Channel  
 BP = Bent Plate  
 SP = Short Plate  
 LP = Long Plate  
 AA = Anchor Angle  
 (2) for location see Figure 7-1

(3) L = Low material properties  
 M = Mean material properties  
 H = High material properties  
 (4) E = Elastic response  
 P = Plastic response  
 (5) LCC removed



TABLE 7-3 Element Loads and Displacements (CASES 1 - 7)

Element No.	Type	CASE 1		CASE 2		CASE 3		CASE 4	
		Load Rm (k)	Displ. Xm (in)	Load Rm (k)	Displ. Xm (in)	Load Rm (k)	Displ. Xr (in)	Load Rm (k)	Displ. Xm (in)
1	LCC	2.608	0.01404	3.416	0.01177	2.489	0.01058	2.876	0.00856
2	BF	2.743	0.03497	2.785	0.03273	2.809	0.03143	3.234	0.02906
3	SP	6.956	0.00655	6.919	0.00651	7.029	0.00662	7.412	0.00698
4	SP	9.560	0.00900	10.325	0.00972	9.514	0.00896	10.286	0.00969
5	SP	11.580	0.01090	12.008	0.01131	10.772	0.01014	11.833	0.01114
6	LP	12.985	0.02445	13.163	0.02479	11.263	0.02530	12.504	0.02558
7	LP	13.750	0.02406	13.752	0.02487	11.269	0.02745	12.509	0.02746
8	LP	13.759	0.02744	13.759	0.02745	11.269	0.02748	12.509	0.02748
9	LP	13.759	0.02748	13.759	0.02748	11.269	0.02748	12.509	0.02748
10	SP	13.759	0.01374	13.759	0.01374	11.269	0.01374	12.509	0.01374
11	AA	4.215	0.02123	4.129	0.01899	4.188	0.01769	4.222	0.01532
12	AA	2.023	0.00931	1.686	0.00775	1.260	0.00580	1.550	0.00451
13	AA	1.407	0.00647	1.157	0.00532	0.479	0.00220	0.657	0.00191
14	AA	0.750	0.00345	0.573	0.00264	0.005	0.00002	0.005	0.00001
15	AA	0.008	0.00004	0.006	0.00003	.000	.00000	.000	.00000
16	AA	.000	.00000	.000	.00000	.000	.00000	.000	.00000
17	AA	.000	.00000	.000	.00000	0.000	0.00000	0.000	0.00000

TABLE 7-3 (continued) Element Loads and Displacements (CASES 1 - 7)

Element No.	Type	CASE 5		CASE 6		CASE 7	
		Load Rm (k)	Displ. Xm (in)	Load Rm (k)	Displ. Xm (in)	Load Rm (k)	Displ. Xm (in)
1	LCC	3.228	0.00767	0.000	0.000	2.482	0.010378
2	BP	3.611	0.02778	2.602	0.042446	2.829	0.030377
3	SP	7.821	0.00736	6.863	0.006462	7.941	0.007477
4	SP	11.041	0.01040	6.863	0.006462	10.554	0.009937
5	SP	12.730	0.01199	9.935	0.009355	12.116	0.011409
6	LP	13.752	0.02492	12.056	0.022705	13.307	0.025061
7	LP	13.759	0.02746	13.142	0.024750	13.705	0.025810
8	LP	13.759	0.02748	13.636	0.025680	13.758	0.027310
9	LP	13.759	0.02748	13.757	0.027000	13.759	0.027474
10	SP	13.759	0.01374	13.759	0.013733	13.759	0.013738
11	AA	4.223	0.01404	4.271	0.028708	3.617	0.016639
12	AA	1.692	0.00432	3.078	0.014157	1.430	0.006578
13	AA	1.007	0.00257	2.125	0.009774	0.924	0.004248
14	AA	0.006	0.00002	1.088	0.005003	0.399	0.001833
15	AA	.000	.00000	0.495	0.002277	0.036	0.000168
16	AA	.000	.00000	0.105	0.000482	.000	0.000002
17	AA	0.000	0.00000	0.001	0.000005	.000	.000000

TABLE 7-4 Comparison of Maximum element response values with capacities for CASE 1  
(see Table 7-1 for definition of element properties)

Member Element Material Response	LCC	BP	SP	SP	LP	AA
	1	2	3	10	9	11
	L	L	L	H	H	L
	P	P	E	P	P	P
Ro	2.124	3.400	11.200	13.690	13.690	4.054
Ry	2.261	2.970	11.250	13.750	13.750	4.200
Ru	5.226	1.150	15.000	17.500	17.500	5.000
Rm	2.608	2.743	6.956	13.759	13.759	4.215
Xy	0.00398	0.02286	0.01059	0.01294	0.02589	0.01932
Xu	0.09001	0.12000	0.76100	0.76300	1.52600	0.12500
Xm	0.01404	0.03497	0.00655	0.01374	0.02748	0.02123
Rm/Ru	0.4991	2.3849	0.4637	0.7862	0.7862	0.8429
Xm/Xu	0.1560	0.2914	0.0086	0.0180	0.0180	0.1698
Um	3.526	1.530	0.618	1.061	1.061	1.099
Uu	22.597	5.249	71.857	58.946	58.946	6.471
Eu	0.327	0.234	9.910	11.810	23.621	0.527
Em	0.029	0.069	0.023	0.100	0.200	0.049
SFe	11.262	3.416	434.987	118.171	118.174	10.833

TABLE 7-5 Comparison of Maximum element response values with capacities for CASE 2  
(see Table 7-1 for definition of element properties)

Member Element Material Response	LCC 1 H P	BP 2 L P	SP 3 L E	SP 10 H P	LP 9 H P	AA 11 L E
R <sub>o</sub>	2.876	3.400	11.200	13.690	13.690	4.054
R <sub>y</sub>	3.113	2.970	11.250	13.750	13.750	4.200
R <sub>u</sub>	9.582	1.150	15.000	17.500	17.500	5.000
R <sub>m</sub>	3.416	2.785	6.919	13.759	13.759	4.129
X <sub>y</sub>	0.00518	0.02286	0.01059	0.01294	0.02589	0.01932
X <sub>u</sub>	0.14612	0.12000	0.76100	0.76300	1.52600	0.12500
X <sub>m</sub>	0.01177	0.03273	0.00651	0.01374	0.02748	0.01899
R <sub>m</sub> /R <sub>u</sub>	0.3565	2.4214	0.4613	0.7862	0.7862	0.8258
X <sub>m</sub> /X <sub>u</sub>	0.0806	0.2728	0.0086	0.0180	0.0180	0.1519
U <sub>m</sub>	2.272	1.432	0.615	1.061	1.061	0.983
U <sub>u</sub>	28.201	5.249	71.857	58.946	58.946	6.471
E <sub>u</sub>	0.903	0.234	9.910	11.810	23.621	0.527
E <sub>m</sub>	0.030	0.062	0.023	0.100	0.200	0.039
SF <sub>e</sub>	30.517	3.755	439.707	118.171	118.174	13.432



TABLE 7-6 Comparison of Maximum element response values with capacities for CASE 3  
(see Table 7-1 for definition of element properties)

Member Element Material response	LCC	BP	SP	SP	LP	AA
	1	2	3	10	9	11
	L	L	L	L	L	L
	P	P	E	P	P	P
Ro	2.124	3.400	11.200	11.200	11.200	4.054
Ry	2.261	2.970	11.250	11.250	11.250	4.200
Ru	5.226	1.150	15.000	15.000	15.000	5.000
Rm	2.489	2.809	7.029	11.269	11.269	4.188
Xy	0.00398	0.02286	0.01059	0.01059	0.02118	0.01932
Xu	0.09001	0.12000	0.76100	0.76100	1.52200	0.12500
Xm	0.01058	0.03143	0.00662	0.01374	0.02748	0.01769
Rm/Ru	0.4762	2.4427	0.4686	0.7512	0.7512	0.8376
Xm/Xu	0.1175	0.2619	0.0087	0.0181	0.0181	0.1416
Um	2.655	1.375	0.625	1.297	1.297	0.916
Uu	22.597	5.249	71.857	71.857	71.857	6.471
Eu	0.327	0.234	9.910	9.910	19.820	0.527
Em	0.020	0.059	0.023	0.095	0.190	0.037
SFe	16.198	3.987	425.982	104.280	104.280	14.215

TABLE 7-7 Comparison of Maximum element response values with capacities for CASE 4  
(see Table 7-1 for definition of element properties)

Member Element Material Response	LCC 1 M P	BP 2 M P	SP 3 M E	SP 10 M P	LP 9 M P	AA 11 M P
Ro	2.528	3.780	12.440	12.440	12.440	4.113
Ry	2.716	3.300	12.500	12.500	12.500	4.200
Ru	7.310	1.520	16.250	16.250	16.250	5.000
Rm	2.876	3.234	7.412	12.509	12.509	4.222
Xy	0.00462	0.02540	0.01177	0.01177	0.02353	0.01222
Xu	0.11750	0.12000	0.76200	0.76200	1.52400	0.12500
Xm	0.00856	0.02906	0.00698	0.01374	0.02748	0.01532
Rm/Ru	0.3934	2.1275	0.4561	0.7698	0.7698	0.8443
Xm/Xu	0.0729	0.2421	0.0092	0.0180	0.0180	0.1225
Um	1.852	1.144	0.593	1.167	1.167	1.254
Uu	25.420	4.724	64.756	64.756	64.756	10.233
Eu	0.572	0.270	10.858	10.858	21.715	0.544
Em	0.017	0.054	0.026	0.098	0.196	0.039
SFe	33.098	5.010	419.749	110.590	110.590	14.063

TABLE 7-8 Comparison of Maximum element response values with capacities for CASE 5  
(see Table 7-1 for definition of element properties)

Member Element Material Response	LCC 1 H P	BP 2 H E	SP 3 H E	SP 10 H P	LP 9 H P	AA 11 H P
R <sub>o</sub>	2.876	4.160	13.690	13.690	13.690	4.125
R <sub>y</sub>	3.113	3.630	13.750	13.750	13.750	4.200
R <sub>u</sub>	9.582	1.900	17.500	17.500	17.500	5.000
R <sub>m</sub>	3.228	3.611	7.821	13.759	13.759	4.223
X <sub>y</sub>	0.00518	0.02794	0.01294	0.01294	0.02589	0.01073
X <sub>u</sub>	0.14612	0.12000	0.76300	0.76300	1.52600	0.12500
X <sub>m</sub>	0.00767	0.02778	0.00736	0.01374	0.02748	0.01404
R <sub>m</sub> /R <sub>u</sub>	0.3369	1.9005	0.4469	0.7862	0.7862	0.8447
X <sub>m</sub> /X <sub>u</sub>	0.0525	0.2315	0.0097	0.0180	0.0180	0.1123
U <sub>m</sub>	1.479	0.994	0.569	1.061	1.061	1.308
U <sub>u</sub>	28.201	4.294	58.946	58.946	58.946	11.647
E <sub>u</sub>	0.903	0.305	11.810	11.810	23.621	0.548
E <sub>m</sub>	0.016	0.050	0.029	0.100	0.200	0.036
SFe	56.620	6.091	410.081	118.171	118.171	15.033

TABLE 7-9 Comparison of Maximum element response values with capacities for CASE 6  
(see Table 7-1 for definition of element properties)

Member Element Material Response	BP 2 L P	SP 3 L E	SP 10 H P	LP 9 H P	AA 11 L P
R <sub>o</sub>	3.400	11.200	13.690	13.690	4.054
R <sub>y</sub>	2.970	11.250	13.750	13.750	4.200
R <sub>u</sub>	1.150	15.000	17.500	17.500	5.000
R <sub>m</sub>	2.602	6.863	13.759	13.757	4.271
X <sub>y</sub>	0.02286	0.01059	0.01294	0.02589	0.01932
X <sub>u</sub>	0.12000	0.76100	0.76300	1.52600	0.12500
X <sub>m</sub>	0.04245	0.00646	0.01373	0.02700	0.02871
R <sub>m</sub> /R <sub>u</sub>	2.2626	0.4575	0.7862	0.7861	0.8543
X <sub>m</sub> /X <sub>u</sub>	0.3537	0.0085	0.0180	0.0177	0.2297
U <sub>m</sub>	1.857	0.610	1.061	1.043	1.486
U <sub>u</sub>	5.249	71.857	58.946	58.946	6.471
E <sub>u</sub>	0.234	9.910	11.810	23.621	0.527
E <sub>m</sub>	0.089	0.022	0.100	0.193	0.080
SFe	2.645	446.894	118.258	122.175	6.556

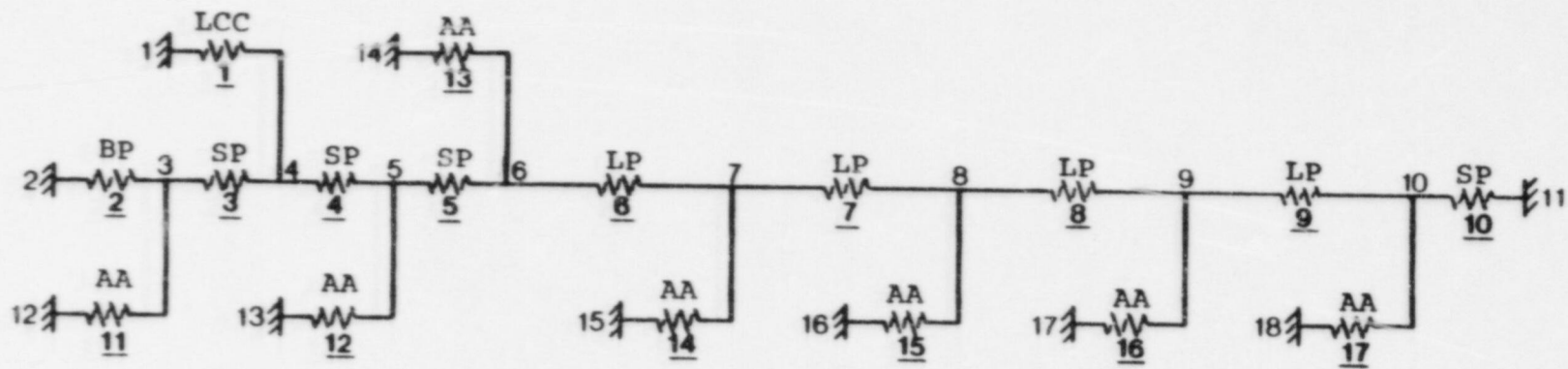


TABLE 7-10 Comparison of Maximum element response values with capacities for CASE 7  
(see Table 7-1 for definition of element properties)

Member Element Material Response	LCC	BP	SP	SP	LP	AA
	1	2	3	10	9	11
	L	L	L	H	H	L
	P	P	E	P	P	E
Ro	2.124	3.400	11.200	13.690	13.690	4.054
Ry	2.261	2.970	11.250	13.750	13.750	4.200
Ru	5.226	1.150	15.000	17.500	17.500	5.000
Rm	2.482	2.829	7.941	13.759	13.759	3.617
Xy	0.00398	0.02286	0.01059	0.01294	0.02589	0.01932
Xu	0.09001	0.12000	0.76100	0.76300	1.52600	0.12500
Xm	0.01038	0.03038	0.00748	0.01374	0.02747	0.01664
Rm/Ru	0.4749	2.4599	0.5294	0.7862	0.7862	0.7235
Xm/Xu	0.1153	0.2531	0.0098	0.0180	0.0180	0.1331
Um	2.605	1.329	0.706	1.061	1.061	0.861
Uu	22.597	5.249	71.857	58.946	58.946	6.471
Eu	0.327	0.234	9.910	11.810	23.621	0.527
Em	0.020	0.056	0.030	0.100	0.200	0.030
SFe	16.602	4.200	333.803	118.171	118.186	17.502

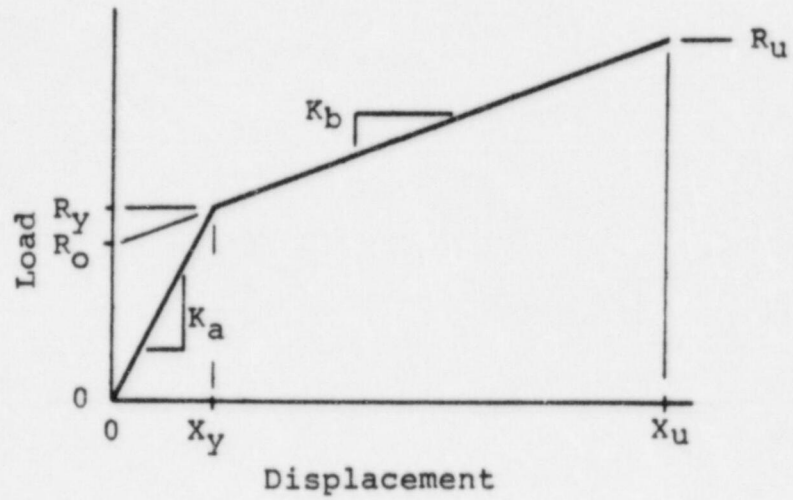
TABLE 7-11 Comparison of Maximum LCC element response values with capacities for CASES 1 - 5 & 7  
(see Table 7-1 for definition of element properties)

CASE	1	2	3	4	5	7
Material	L	H	L	M	H	L
Response	P	P	P	P	P	P
Ro	2.124	2.876	2.124	2.528	2.876	2.124
Ry	2.261	3.113	2.261	2.716	3.113	2.261
Ru	5.226	9.582	5.226	7.310	9.582	5.226
Rm	2.608	3.416	2.489	2.876	3.228	2.482
Xy	0.00398	0.00518	0.00398	0.00462	0.00518	0.00398
Xu	0.09001	0.14612	0.09001	0.11750	0.14612	0.09001
Xm	0.01404	0.01177	0.01058	0.00856	0.00767	0.01038
Rm/Ru	0.4991	0.3565	0.4762	0.3934	0.3369	0.4749
Xm/Xu	0.1560	0.0806	0.1175	0.0729	0.0525	0.1153
Um	3.526	2.272	2.655	1.852	1.479	2.605
Uu	22.597	28.201	22.597	25.420	28.201	22.597
Eu	0.327	0.903	0.327	0.572	0.903	0.327
Em	0.029	0.030	0.020	0.017	0.016	0.020
SFe	11.262	30.517	16.198	33.098	56.620	16.602

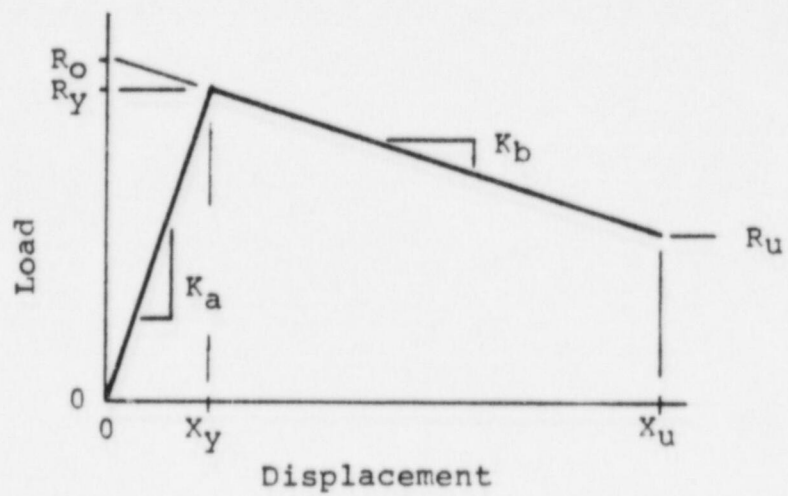


<u>Element</u>	<u>ID</u>	<u>Description</u>
LCC	<u>1</u>	Leak Chase Channel
BP	<u>2</u>	Bent Plate (L = 7½")
SP	<u>3,4,5,10</u>	Short Plate (L = 7½")
LP	<u>6-9</u>	Long Plate (L = 15")
AA	<u>11-17</u>	Angle Anchors

Figure 7-1 Mathematical Model for Dome Liner Plate Section



Resistance Function for LCC, Straight Plate and Angle Anchors



Resistance Function for Bent Plate

Figure 7-2 Resistance Functions for Limer Plate Component Springs



## 8.0 INTERIOR LCC SECTION AND TEST TUBING ANALYSES

### 8.1 LCC SECTION SELECTION

Interior LCC sections occur in all areas of the containment liner plate. The location and description of typical interior LCC sections are shown in Table 5-1. Typical configurations are shown in Figure 5-6.

As indicated in Table 5-1, typical LCC sections were used in several details throughout the liner plate system. In cases where the LCC geometry remained unchanged, selection of a particular section for analysis was based on the most severe loading condition for that application group (Sections 1, 4, 5 through 9, and 13).

Where geometry changes occurred within an application group (such as changes in LCC plate section thicknesses or lengths), selection of sections for analysis were based on most severe geometry as well as severity of loading conditions (Sections 2, 3, 11, and 12).

This selection procedure minimized the number of sections subjected to analysis to assess the severity of loading on the interior LCCs.

### 8.2 LOADING CONDITIONS

The LCC sections receive direct containment internal pressure load (60 psig accident pressure controls) in addition to forced displacements due to the strain in the structural elements (liner plate, penetrations, etc) to which the LCC members are attached. The maximum relative liner plate strains used in the interior LCC analyses are given and discussed in Section 6.0. These strains reflect average strains in the 1/4-inch-thick liner plate. These strain levels are altered locally in the

vicinity of liner plate thickness changes, penetrations, bracket locations, etc. These local changes in strain levels have been accounted for in the LCC analyses. Strain levels due to other applied loads (such as pipe reaction strains at Section 12) have also been accounted for.

### 8.3 ANALYTICAL APPROACH

In addition to direct pressure loading, the LCC members are subjected to both induced axial strains (along the axis of the LCC) and lateral displacements at the attachment points to the supporting structural elements (e.g., liner plate or penetration).

The axial strain in the LCC is comparable to the strain in the supporting element in the axial direction of the LCC. The lateral displacement of the LCC member support points is a direct function of the distance between the support points and the support element strain transverse to the LCC axis. Additional relative lateral displacements are induced by the Poisson effect associated with the axial LCC strain. These forced lateral displacements induce internal forces and moments into the LCC member cross section which responds to these displacements essentially as a rigid frame (flexural continuity at corners and support points).

The response to direct pressure loading will again be essentially as a rigid frame (or arch as in the case of pipe sections LCCs in Section 10 of Figure 5-6).

The axial LCC stresses and strains will be comparable to those of the support element in the axial direction of the LCC. In no known internal LCC case can they be more severe. Therefore, further analyses in the axial direction is not required. (The adequacy of all supporting elements has previously been

determined in original plant documents and is therefore out of the scope of this investigation.)

Investigation of the adequacy of the LCC members cross sections (and attachment welds) to withstand the external pressure loading and forced lateral displacements involved the following general procedure:

- a. Define axial and transverse strains in supporting elements.
- b. Determine direct pressure loads.
- c. Set up frame model for LCC section (see Figure 8-1).
- d. Determine forced displacements due to transverse and axial strains ( $\Delta 1$  and  $\Delta 2$  in Figure 8-1).
- e. Solve frame model for internal moments and forces (and strain levels where required) in the LCC members and attachment welds.
- f. Assess adequacy of LCC based on section capacities and acceptable strain limits.

Conventional structural analysis procedures were utilized in solving the frame models. For analytical purposes, the supporting structural elements were assumed to remain elastic. This is the most severe case since any yielding of the support members would diminish internal LCC moments and forces. In cases where inelastic response was predicted, ductility ratios based on strain levels and plastic section strengths were calculated.

Assessment of severity of loading is based on comparisons of calculated moment versus moment capacity and response ductility ratios.

#### 8.4 RESULTS OF ANALYSES

The results of the analyses of the selected internal LCC sections are summarized in Table 8-1.

The calculated moments at the critical section reflect the response to the forced displacements plus a direct accident pressure of 60 psig. For all cases, the critical section was through the throat of the fillet welds. In all cases, except for Sections 11 and 12, the critical weld location was at the LCC-to-support-member joint. For Section 11, critical stresses were reached at the supports and at the joint between 1/4-inch LCC plates. For Section 12, the critical section was at the joint between the 1/4-inch LCC plates.

The throats of the 3/16-inch fillet welds were the most critically stressed areas because they have the thinnest cross section with a section modulus of half of that for the next thinnest LCC member used (L 1 x 1 x 3/16). Although the weld metal is typically stronger (minimum yield stress of 50 ksi) than the ASTM A 36 LCC members (minimum yield stress of 36 ksi) by a ratio of 1.39, this material strength difference is insufficient to counter the two-to-one minimum difference in section modulus.

The LCC sections were found to remain elastic (based on plastic section strength limit) for all cases except for Sections 3a and 3c.

The higher moments at Section 3a are primarily due to a short stiff leg (1-1/2 x 3/8 PL) being displaced by the relatively long (3-1/2 x 3/8) leg. At other locations, section thicknesses were 1/4-inch or less with maximum length dimensions on the order of 2 inches. The plate length and thickness effect can be seen by comparing Section 3a with 3b which is subjected to similar loading. The higher moments at Section 3c are due to



the larger forced displacement (0.00674 inch versus 0.00216 inch) and greater restraint provided by the thickened liner plate for multiple penetrations located away from an exterior thickened plate edge.

The resulting maximum ductility ratio of 1.94 is well within acceptable range. Strain limits of 50% of the strain at ultimate stress are considered acceptable. For this case, ultimate stress is considered at a strain limit of 10% (one-half of minimum % elongation). This results in a calculated maximum ductility ratio (at ultimate stress) of 43. The corresponding acceptable ductility ratio would be 21.5, which is much greater than the predicted value of 1.94.

Based on the foregoing analytical results, the interior LCC sections are structurally capable of withstanding the applied loading with considerable reserve deformation capacity.

#### 8.5 BASE LCC SECTION CLEARANCE CHECK

The 1/2-inch styrofoam placed around the base LCCs (and test pipes) prior to placing upper slab concrete (see Figures 5-5 and 5-6) provides protection against interference between the LCC and the upper slab sections due to relative displacement.

The magnitude of relative displacement between the LCCs and the upper slab sections is a function of the unrelieved length of the upper slab (between an expansion joint and an effective anchor or another expansion joint). The locations of expansion joints separating the upper slab sections are shown in Figure 8-2. Figure 8-2 also shows the longest unrelieved section with an unrelieved length of approximately 20 feet (extending each way from the vicinity of Column A to the perimeter expansion joints). The dead load from Column A inhibits relative movement near the column. This results in an effective anchor at this location.

The maximum calculated relative displacement between the LCCs and the upper concrete slab is 0.36 inch based on an estimated average temperature difference of 231F (1,500  $\mu$ ) between the upper and lower slabs and an unrelieved 20-foot length of upper slab. The 1/2-inch gap between the LCC and the concrete formed by the styrofoam spacers (shown in Figure 5-3) is sufficient to prevent channel-to-concrete contact. Styrofoam in this configuration can be compressed to less than 10% of its initial thickness without significant load transfer. A minimum effective gap of approximately 0.45 inch is available to accommodate the maximum predicted relative displacement of 0.36 inch. The LCCs would therefore not be subjected to direct loading through interaction with the concrete.

The LCCs would only be subjected to flexurally induced elastic strains from minor deformation of the concrete slabs due to the effects of pressure and overall thermal gradients as covered in Section 8.4.

## 8.6 TEST PIPES

### 8.6.1 Test Pipes for Exterior LCCs

The test pipes for the exterior LCCs (embedded in concrete primarily in the dome area) are welded directly to the liner plate. The test pipes have sufficiently thick walls to preclude buckling from externally applied containment accident design pressure (60 psig).

The interface of the test pipe to the liner plate is subjected to the same magnitude of induced strain (from applied mechanical and thermal loads) as the liner plate. The liner plate steel (ASTM A 442) and the test pipe (ASTM A 333) have similar ductile properties and are joined by compatible weld material (E60 or E70 rods). Therefore, no cracking or material failures are expected at these connections.

### 8.6.2 Test Pipes for Interior LCCs

The test pipes for interior LCCs (in the lower dome, shell, cone, base, and pit areas) are welded directly to the LCC angle legs or to the webs of the channel sections. These connections are less severely strained than the exterior LCC test pipe connections as a result of strain relief afforded by deformation of the angle and channel legs.

The test pipes extending through the upper concrete slabs in the base and pit areas are protected from direct damage at the pipe-to-LCC connection by the 1/2-inch thick styrofoam spacer material which extends to 12 inches from the liner plate.

Relative motion between the slab and the liner plate can induce a maximum flexural rotation of 0.03 radians. This is much less than the 0.265 radian leaktight weld joint rotations observed in the tests described in Appendix B (also see discussion in Section 9.0). Therefore, leakage should not occur in these test pipes or in their connections to the LCCs.

TABLE 8-1 - SUMMARY OF INTERIOR LCC SECTION ANALYSES

Section ID <sup>(1)</sup>	LCC Member	Forced Displacement (in.)	Critical Section <sup>(2)</sup> Location	Calculated Moment <sup>(3)</sup> (in. #/in.)	Ductility Ratio <sup>(4)</sup> (U <sub>m</sub> )	Notes
1	C 2x9/16x3/16	0.002418 each leg	(5)	118	<1	(8)
2	C 2x9/16x3/16	0.002046 each leg	(5)	100	<1	(8)
3a <sup>(10)</sup>	1-1/4x3/8 PL 3-1/2x1/4 PL	0.00216 @ 1-1/2-inch leg	(5)	203	1.03	(9)
3b <sup>(10)</sup>	1-1/2x1/4 PL 3-1/2x1/4 PL	0.00216 @ 1-1/2-inch leg	(5)	48.6	<1	(8)
3c <sup>(11)</sup>	1-1/2x1/4 PL 3-1/2x1/4 PL	0.00674 @ 1-1/2-inch leg	(5)	384	1.94	(9)
4	See Note 12					
5	L 1x1x3/16	0.00231 each leg	(5)	193	<1	(8)
6	L 1x1x3/16	0.00160 each leg	(5)	121	<1	(8)
7	C 2x9/16x3/16	0.00160 each leg	(5)	79	<1	(8)
8 & 9	L 1x1x3/16	0.00160 vert. leg	(5)	121	<1	(8)
10	2-1/2-inch diameter pipe section	0.00113 each support	(5)	10	<1	(8)
11	2-1/2-inch diameter pipe section	0.00144 each support	(6)	16	<1	(8)
12	2x1/4 PL 3x1/4 PL	0.0019 @ 2-inch leg	(7)	60	<1	(8)
13	C 2x9/16x3/16	0.00238 each leg	(5)	116	<1	(8)

## Notes:

- (1) For location and description of LCC sections see Table 5-1 and Figure 5-6.
- (2) The critical section for all LCCs was through the throat of the 3/16-inch fillet welds. These welds have a moment capacity of 198 in.-lb/in. based on the plastic section modulus and a yield strength of 45 ksi (0.9 f<sub>y</sub>, where f<sub>y</sub> = 50 ksi - minimum ASTM-specified value). See Table 5-2 for liner plate and LCC physical properties.
- (3) Calculated moments are based on assumed elastic behavior. Where calculated moments exceed 198 in.-lb/in. as discussed in Note 2, a ductility ratio greater than 1 is indicated. Calculated moments reflect the combined effect of forced displacements plus an internal accident pressure of 60 psi.
- (4) The ductility ratio is the ratio of the maximum calculated displacement to the yield displacement based on the section strength discussed in Note 2. Linear behavior to yield is assumed.
- (5) At 3/16-inch fillet weld joining LCC member to liner plate (see Note 2).
- (6) At 3/16-inch fillet welds at split pipe-to-1-inch cone joints.
- (7) At 3/16-inch fillet weld joining 1/4-inch LCC plates.
- (8) Section remains elastic.
- (9) Section at weld(s) plastic (U<sub>m</sub> > 1), all other sections remain elastic.
- (10) For LCCs associated with a single isolated electrical penetration or for LCC sections closest to the edge of the thickened plate for multiple electrical penetration clusters.
- (11) For LCCs associated with multiple electrical penetration clusters located away from (interior) thickened plate edge.
- (12) LCC section behavior is essentially the same as for Section 1. Out-of-plane reaction resisted by embedded channel section.



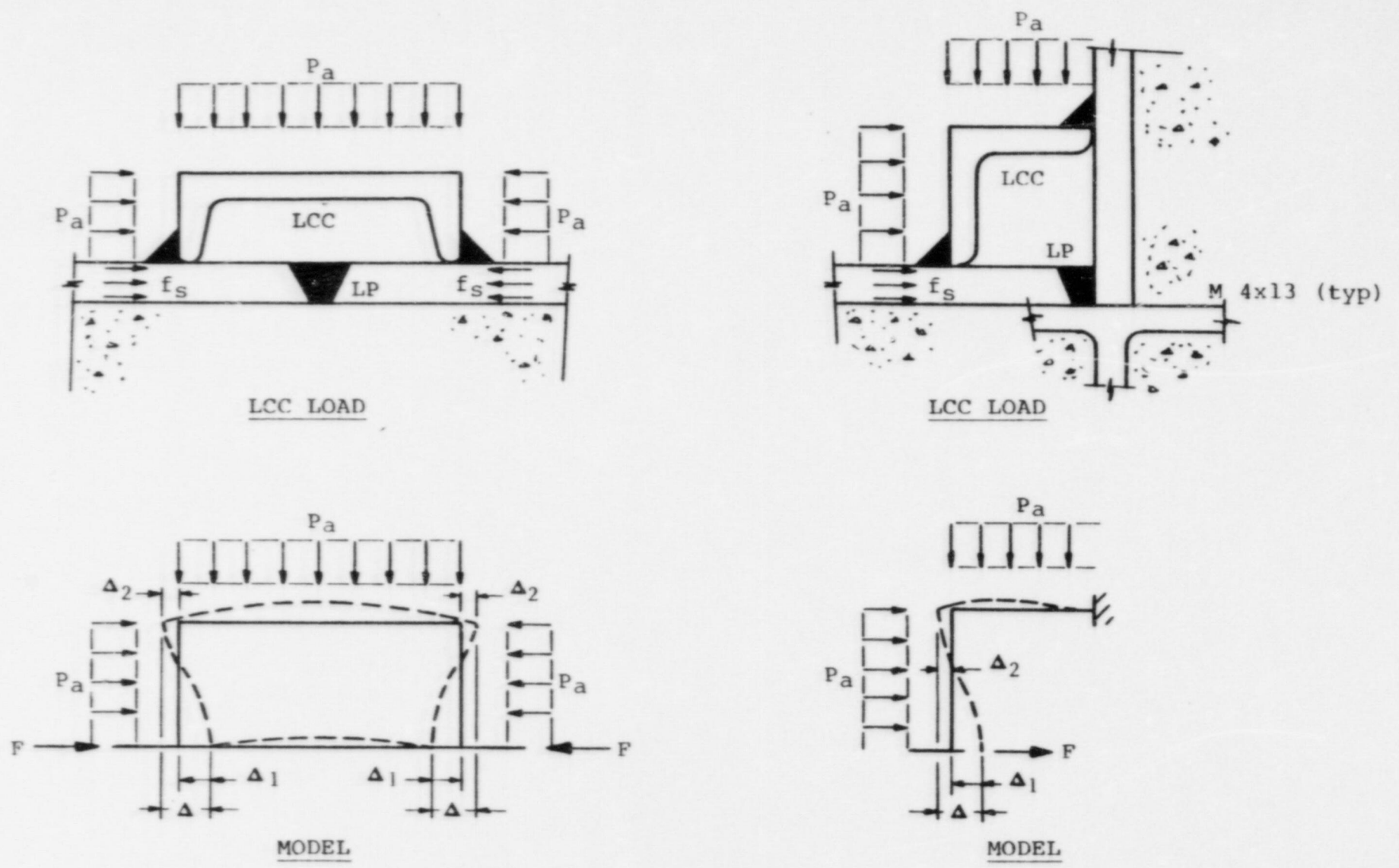


Figure 8-1 Typical LCC Loading and Models

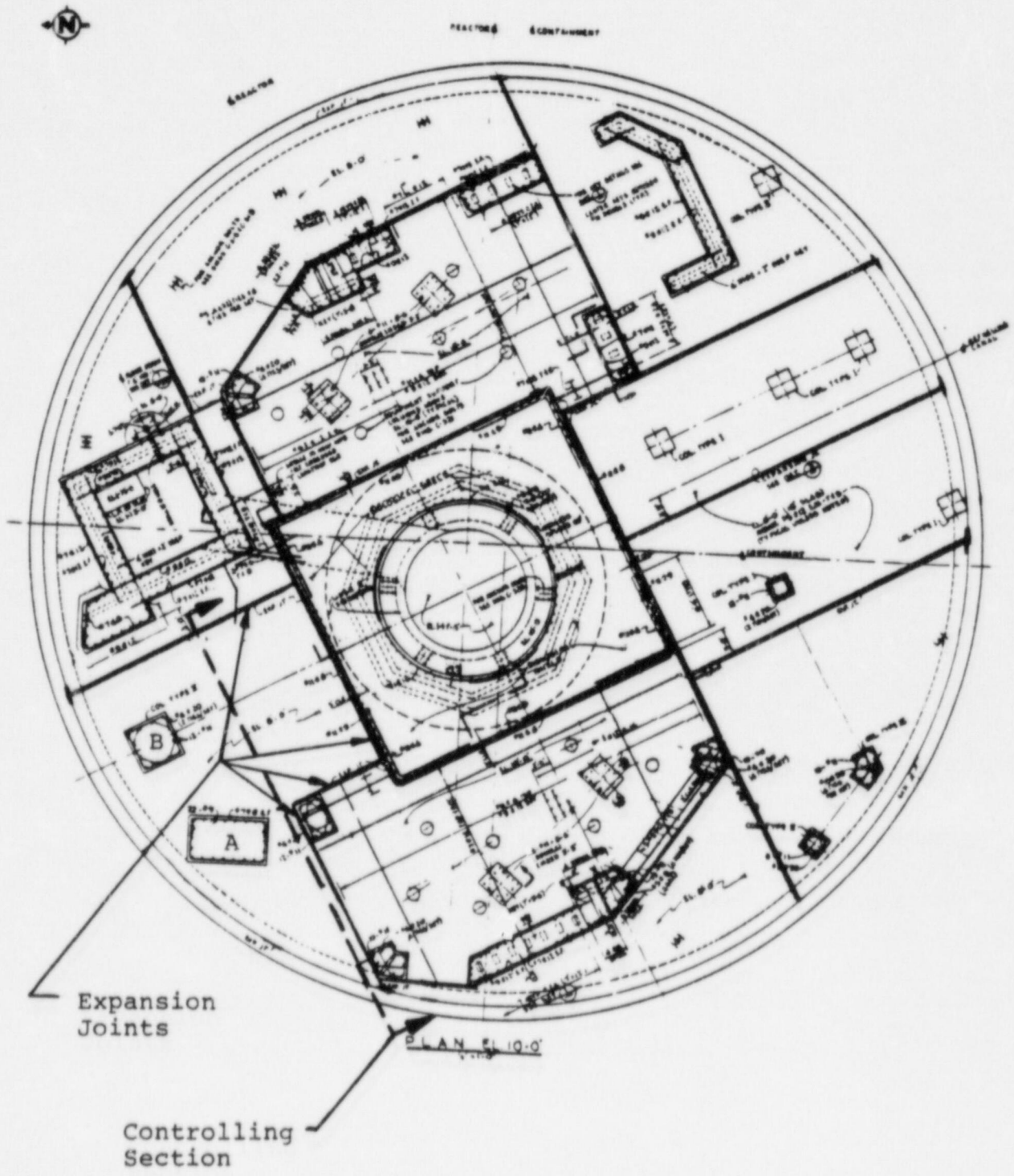


Figure 8-2 Location of Base Liner Plate Controlling Section

## 9.0 LEAKTIGHT INTEGRITY

Leaktight integrity is a specified requirement for the LCC system (Specification No. 6118-C-7, Reference 7). Reference 7 requires that the LCCs be soap bubble tested and pressure decay tested under a test pressure of 70 psig. Any leaks discovered were required to be repaired until all LCCs successfully past the leak tests. Construction records discussed in Section 4.0 confirm that these requirements were met.

Additional leak tests (Reference 8) were performed in support of this investigation to confirm leaktight integrity under severe transverse load conditions (test descriptions and results are summarized in Appendix B). The tests demonstrated that the LCCs (and the 3/16-inch double pass fillet welds) retained their leaktight integrity throughout the test loading which produced lateral deformations (in the 2-inch channel sections) in excess of 0.149 inch. This corresponds to a joint rotation at the attachment welds on the order of 0.265 radians (over 15°).

The maximum calculated resistance for dome section LCCs is 3.42 k/in. of plate (Table 7-11, Case 2). This corresponds to an elastic LCC steel displacement of 0.00475 inch (based on steel LCC elastic stiffness of 720 k/in. from Appendix B) or 3.2% of the measured deformation producing no leaks.

The maximum calculated leg displacement (forced) for interior 2-inch channel LCCs is 0.002418 inch (Table 8-1, Section 1). This corresponds to 1.6% of the measured deformation producing no leaks.

The maximum rotation for other interior LCCs is 0.0045 radians (Table 8-1, Case 3c, an 0.00674-inch displacement on a 1-1/2-inch-long leg).

This corresponds to 1.7% of the measured rotation (at weld) producing no leaks.

The dome LCC, Load Case 2, at 3.2% of the measured no leak displacement is therefore the controlling condition with respect to deformation or rotation.

The test data combined with the calculated displacements show that there is considerable margin between calculated displacements and the leaktight displacements verified by testing. Therefore, no leakage is expected at these relatively low displacement levels.



## 10.0 OVERALL ASSESSMENT

Assessment of the acceptability of utilizing the LCC system as part of the pressure boundary involves several factors such as:

- a. Liner plate system performance history
- b. QA/QC measures during construction
- c. Construction records indicating evidence of conformance with drawings and specifications
- d. Structural behavior and severity of loading on LCCs
- e. Confirmation of leaktight integrity by tests, analyses, and quality control and historical records

The results of this investigation with respect to the above factors are summarized and evaluated in the following subsections.

### 10.1 PERFORMANCE HISTORY

The performance history summarized in Section 3.0 indicates that 49 plants have similar liner plate systems. In over 400 reactor years of combined operating experience at these plants over 100 post-startup ILRTs have occurred with no known leaks in either the liner plate butt welds or the LCCs. Some of the plants (such as Surry Units 1 and 2 and North Anna Units 1 and 2) are operated at subatmospheric pressures which essentially constitutes over 34 years of liner plate system leak testing under a continuous partial vacuum.

In other cases such as Beaver Valley Unit 1, the plant was operated with the LCC system pressurized to approximately

80 psi. This constitutes a continuous leak test of the LCC system as well as the liner plate butt welds.

## 10.2 QUALITY OF CONSTRUCTION

Specification 6118-C-7 (Reference 7) for furnishing, fabrication, delivery, and erection of the containment structure liner plate and accessory steel contains similar requirements for both the LCCs and the liner plate and attachments. For example:

- a. Mill certifications are required for material
- b. Welders must be qualified
- c. Inspection requirements are specified.
- d. Pressure boundary welds (e.g., LCC fillet welds and liner plate butt welds) are required to be double pass welds.
- e. Vacuum box testing is required for the liner plate butt welds while both pressure decay and soap bubble leak tests are required for the LCC system.

A review of construction records shows that the specified quality control measures were enforced and the required testing and inspections were performed (see Section 4.0). Also, Bechtel design and vendor drawings appeared to be in agreement. Therefore, it is concluded that the liner plate and LCC system were constructed, inspected, and tested as designed and specified.

### 10.3 STRUCTURAL EVALUATION

Tests reported in Reference 8 and summarized in Appendix B, confirm the load and deformation capacities of the LCCs. The least LCC factor of safety based on strain energy (and test-defined capacities) for external LCCs (embedded in concrete) was determined in Section 7.0 to be greater than 11. This value reflects the most severe loading and materials properties combinations. The most severe conditions for the interior LCCs resulted in a ductility ratio of 1.94 (Section 9.0). This is comparable to a safety factor based on displacement of about 22. These relatively large calculated safety factors, along with conservative analytical assumptions, would rule out loss of function through structural distress associated with the postulated loading conditions. The structural analyses show that overall structural safety margins for the liner plate system are improved by the presence of the LCCs, particularly in the dome section.

The analyses and tests demonstrate that the LCCs are rugged components and well suited to function as integral parts of the liner plate system.

### 10.4 LEAKTIGHT INTEGRITY

The leaktight integrity of the LCC system was confirmed by test during construction (Section 4.0). The combined liner plate - LCC system leak integrity has been confirmed in subsequent integrated leak rate tests. Other plants have had similar favorable performance (Sections 3.0 and 10.1). Additional leakage tests were performed which confirm leaktight integrity under severe load and deformation conditions (Reference 8). These tests are also discussed in Section 9.0 and Appendix B).

All tests, analyses, and quality control and historical records indicate that the liner plate LCC systems will retain their

leaktight integrity under the most severe postulated loading conditions.

#### 10.5 CONCLUSION

Considering the positive aspects of all the foregoing factors, it is concluded that the liner plate LCC system is well suited to function as a part of the containment structure pressure boundary.



## 11.0 REFERENCES

1. Final Safety Analysis Report, Point Beach Nuclear Plant Units 1 and 2, Wisconsin Electric Power Company
2. World List of Nuclear Power Plants, Operable, Under Construction, or On Order (30 MWe and Over) as of December 31, 1984, Nuclear News-American Nuclear Society, Volume 28/No. 2 (February 1985)
3. Commercial Nuclear Power Plants, NUS Corporation, 17th Edition (February 1985)
4. T.E. Johnson and B.W. Wedellsborg, Containment Building Liner Plate Design Report, Bechtel Topical Report BC-TOP-1, Revision 1 (December 1972), Bechtel Power Corporation
5. D. Pirtz, Studies of Concrete for Two Rivers Nuclear Containment Vessel, Progress Report 2 (August 5, 1969), University of California, Berkeley
6. Reactor Containment Leakage Testing for Water-Cooled Power Reactors, 10 CFR 50 Appendix J, U.S. Nuclear Regulatory Commission (September 1980)
7. Specification for Furnishing, Fabrication, Delivery, and Erection of Containment Structure Liner Plate and Accessory Steel for the Point Beach Nuclear Plant Units No. 1 and 2, Specification No. 6118-C-7, Bechtel Corporation, San Francisco, California for Westinghouse Electric Corporation, Atomic Power Division, original issue January 12, 1967
8. Hiltunen, D.R., et al, Test Report on Static Load Tests on Liner Plate Leak Chase Channel Assemblies, University of Michigan Civil Engineering Department for Bechtel Power Corporation, December 1985
9. Letter, J.Z. LaPlante of WPECo to T.W. Vanvick of Bechtel, Subject: Leak Chase Channel Test Connection Evaluation, March 4, 1986
10. Trip Report, M. Reifschneider to Point Beach Nuclear Plant, April 22, 1986

APPENDIX A

NOTATION

APPENDIX A

NOTATION

<u>Symbol</u>	<u>Definition</u>
AA	Anchor angle
BP	Bent plate
C	Creep load
D	Dead load
$\Delta P$	Differential pressure load
E	Elastic response
$E_c$	Elastic modulus for concrete (ksi)
$E_m$	Strain energy at maximum response (in.-k)
$E_o$	Operating basis earthquake
$E_s$	Elastic modulus of steel (ksi)
$E_u$	Strain energy at ultimate load and/or displacement (in.-k)
$E'$	Seismic DBE (design basis earthquake)
$f_c$	Concrete compressive strength (ksi)
$f_s$	Steel stress (ksi)
$f_y$	Steel yield strength (ksi)
$f_u$	Steel ultimate strength (ksi)
H	High material strength properties
$K_a$	Spring constant for elastic portion of load- displacement function (k/in.)
$K_b$	Spring constant for plastic portion of load- displacement function (k/in.)
$K_c$	Concrete stiffness (k/in.)
$K_s$	Steel LCC section stiffness (k/in.)
$K_t$	Combined concrete and steel LCC stiffness (k/in.)
L	Low material strength properties
LCC	Leak chase channel (including test pipe)
LP	Long plate, 15-inch-long section of liner plate
M	Mean material strength properties
P	Plastic response

<u>Symbol</u>	<u>Definition</u>
$P_a$	Accident pressure
$P_s$	Prestress load
$R_o$	Load axis intercept of plastic portion of load-displacement curves (k)
$R_m$	Element resisting force at maximum response to applied load (k)
$R_y$	Yield load capacity (k)
$R_u$	Ultimate load capacity (k)
S	Shrinkage load
$SF_e$	Safety factor based on strain energy
SP	Short plate
$T_a$	Accident thermal load
$T_c$	Average temperature of concrete (°F)
$T_{max}$	Maximum temperature inside containment (°F)
$T_o$	Operating thermal load
$\mu$	Microstrain ( $10^{-6}$ in./in.)
U	Load combination
$U_m$	Ductility ratio at maximum response ( $X_m/X_y$ )
$U_u$	Ductility ratio at ultimate displacement or maximum available ductility ratio ( $X_u/X_y$ )
$X_m$	Displacement at maximum response to applied load (in.)
$X_y$	Yield displacement (in.)
$X_u$	Ultimate displacement (in.)



APPENDIX B  
LINER PLATE  
LEAK CHASE CHANNEL  
TESTS

## APPENDIX B

### LINER PLATE LEAK CHASE CHANNEL TESTS

#### B1.0 INTRODUCTION

For other than straight plate or outward curvature liner plate, the load versus displacement characteristics of other liner plate elements have been established by tests such as discussed in Reference 4. The load versus displacement functions for the short plate, and long plate, elements were determined from the liner plate material's physical properties. A combination of physical properties and test data were utilized, along with the procedures contained in Reference 4, to define the load versus displacement functions for the bent plate and anchor angles.

The leak chase channel (LCC) sections were not considered in previous analyses as essential elements in restraining liner plate movements and, as a consequence, they have not previously been investigated experimentally. It was, therefore, necessary to devise the set of tests documented in Reference 4 to obtain the necessary data to enable inclusion of these elements in the present liner plate analyses.

In addition to obtaining load-deformation data, the test were conducted with the LCCs pressurized with air to confirm leaktight integrity under the severe load and deformation conditions imposed during testing.

A summary description of these tests along with selected data and results are contained in the following subsections (for reader information and convenience). Only information utilized directly in this report is included. For a detailed description of all test and equipment and a compilation of all test data, see Reference 8.

## B2.0 DESCRIPTION OF TESTS

### B2.1 TEST SPECIMENS

The tests reported in Reference 8 included tests on both composite liner plate LCC specimens embedded in concrete and steel-only specimens. Descriptions of the two specimen types are given in Figures B2-1 and B2-2.

### B2.2 TEST ARRANGEMENTS

Test arrangements for testing the two specimen types are shown in Figures B2-3 and B2-4. Notation used to identify test components is given in Table B2-1.

For the composite tests (Figure B2-3), the embedded LCCs were loaded in transverse shear by calibrated hydraulic rams ( $G_1$  and  $G_2$ ) pressurized by pumps PV1 and PV2. Loads were transferred from the rams to the specimens through a counter-weighted pull beam (D). Loads were determined from calibrated pressure gage (P1 and P2) readings. Displacements were measured by dial gages mounted to the dial gage support assembly, K. LCC air pressure was monitored during the test by air pressure gages J1 and J2.

For the independent steel liner plate LCC tests (Figure B2-4) the specimens (A and B) were loaded by a compression testing machine platen bearing on loading fixture E. Fixture E engaged the LCCs directly in line with the LCC webs. Applied load was measured directly by the testing machine. Dial gages (D1 and D2) measured the relative displacement between the liner plate and the web of the LCC sections (load point). Again, LCC air pressures were monitored by air pressure gages J1 and J2.



## B2.3 TEST RESULTS

### B2.3.1 Materials Properties

The physical properties of the specimen materials are summarized in Table B2-2. The steel properties were determined from tests on samples taken from the material from which the test specimens were fabricated. These confirmatory values are in agreement with the values in the Certified Material Test Reports (CMTRs) furnished by the material suppliers. The concrete strength corresponds to the average concrete test block strength at the time of testing. Other concrete properties correspond to the 28-day test values.

### B2.3.2 Load Displacement Data

#### B2.3.2.1 Composite Tests

A summary of the first crack and ultimate load and displacement data for the composite tests is given in Table B2-3. The first crack data give an indication of the onset of nonlinear behavior attributable to localized cracking in the immediate vicinity of the LCC bearing area.

The ultimate load data defines the prefailure limits for normal bearing interaction behavior of the LCC.

A summary of the composite specimen shear load and displacement test data are contained in Table B2-4. These data define the specimen behavior from no load through the bearing mode limit and include some data points in the shear friction response mode (phase). Plots of data points and development of bearing mode resistance functions based on these data are contained in Section B3.0. In all tests, the limiting failure mode was bearing failure of the concrete compressed by the engaged leg of the LCC. There were no discernible permanent deformations of



the LCCs (due primarily to high LCC yield stress - see Table B2-2).

#### B2.3.2.2 Steel Liner Plate LCC Tests

The independent steel liner plate LCC load versus displacement data are summarized in Table B2-5. Plots of data points and development of steel-controlled load versus displacement functions are contained in Section B3.0.

No physical steel LCC section failures were observed in any of these tests. The tests were terminated due to displacement limits of the test fixtures. Sufficient data were acquired to fully define the positive slope portions of the specimen resistance functions.

#### B2.3.2.3 Combined Data

The combined data from these two sets of tests enabled definition of bilinear spring properties for LCC elements considering variations in both steel and concrete strength properties (see Section B3.0).

#### B2.3.3 Leak Test Data

For both the composite and the independent LCC tests, leaktight integrity of the LCC sections and welds was maintained throughout all phases of testing. The LCCs were pressurized with air at  $65 \pm 5$  psi. This pressure level was maintained throughout the load tests except for specimen S-IIA which developed a leak in the end seals. A leak test was performed on this specimen after the load test was completed which also confirmed its leaktight integrity.

No LCC failures could be produced within the displacement limits of the test arrangement. Displacements of 0.245 and 0.149 inch

were reached in independent steel liner plate LCC Tests I and II. These displacements correspond to joint rotations of 0.436 and 0.265 radians (or 25 and 15 degrees) respectively. Maintaining leaktightness throughout these relatively high test displacements and rotations gives an indication of the integrity on the 3/16-inch double pass fillet welds used throughout the LCC system to attach the LCC members to supporting plate or other elements.

For comparisons with calculated displacements and rotations, see Section 9.0.

TABLE B2-1 - TEST COMPONENT LEGEND

COMPOSITE TESTS

A	Concrete block with embedded LCCs
B	Bearing plate
C	Tie rod system
D	Pull beam
E	Counterbalance assembly
F	High strength bolts
G1	Hydraulic ram
G2	Hydraulic ram
H	Shims
I1	Air line block valve
I2	Air line block valve
J1	Air pressure gage
J2	Air pressure gage
K	Dial gage support assembly
L	Retainer bolts (removed before testing)
P1	Hydraulic pressure gage
P2	Hydraulic pressure gage
PV1	Hydraulic pump
PV2	Hydraulic pump

STEEL TESTS

A	Steel liner plate LCC specimen
B	Steel liner plate LCC specimen
C	Spacer block
D	Lower retainer bolts
E	Loading plate
F	Upper retainer bolts
I1	Block valve in air line to Specimen A
I2	Block valve in air line to Specimen B
J1	Air pressure gage for Specimen A
J2	Air pressure gage for Specimen B

TABLE B2-2 Specimen Strength Properties

STEEL ITEMS			
Component	Yield Strength (fy, ksi)	Ultimate Strength (fu, ksi)	Percent Elongation
1/4" Liner Plate	45.8	68.4	37.5
C2x9/16x3/16	61.6	79.8	25.7

CONCRETE TEST BLOCK

Compressive Strength * (f'c)	4.74 ksi
Elastic Modulus (Ec)	4,180 ksi
Poisson's Ratio (u)	0.13

\* Average Strength at time of testing



TABLE B2-3 Summary of First Observed Crack and Ultimate Load and Displacement Data for Composite Tests

Specimen	FIRST CRACK			ULTIMATE LOAD		
	Shear Load (kips)	Displacement Vert. (in.)	Displacement Horiz. (in.)	Shear Load (kips)	Displacement Vert. (in.)	Displacement Horiz. (in.)
I.A	24.85	0.0161	0.0017	49.50	0.082	0.212
I.B	24.71	0.0112	0.0011	51.88	0.080	0.242
II.A	21.83	0.0083	0.0006	58.05	0.110	0.240
II.B	21.70	0.0060	0.0004	52.27	0.045	0.061
III.A	21.83	0.0080	0.0006	40.15	0.042	0.055
III.B	21.70	0.0040	0.0002	45.32	0.053	0.062

TABLE B2-4

## Shear Load versus Displacement Data for Composite Test Specimens

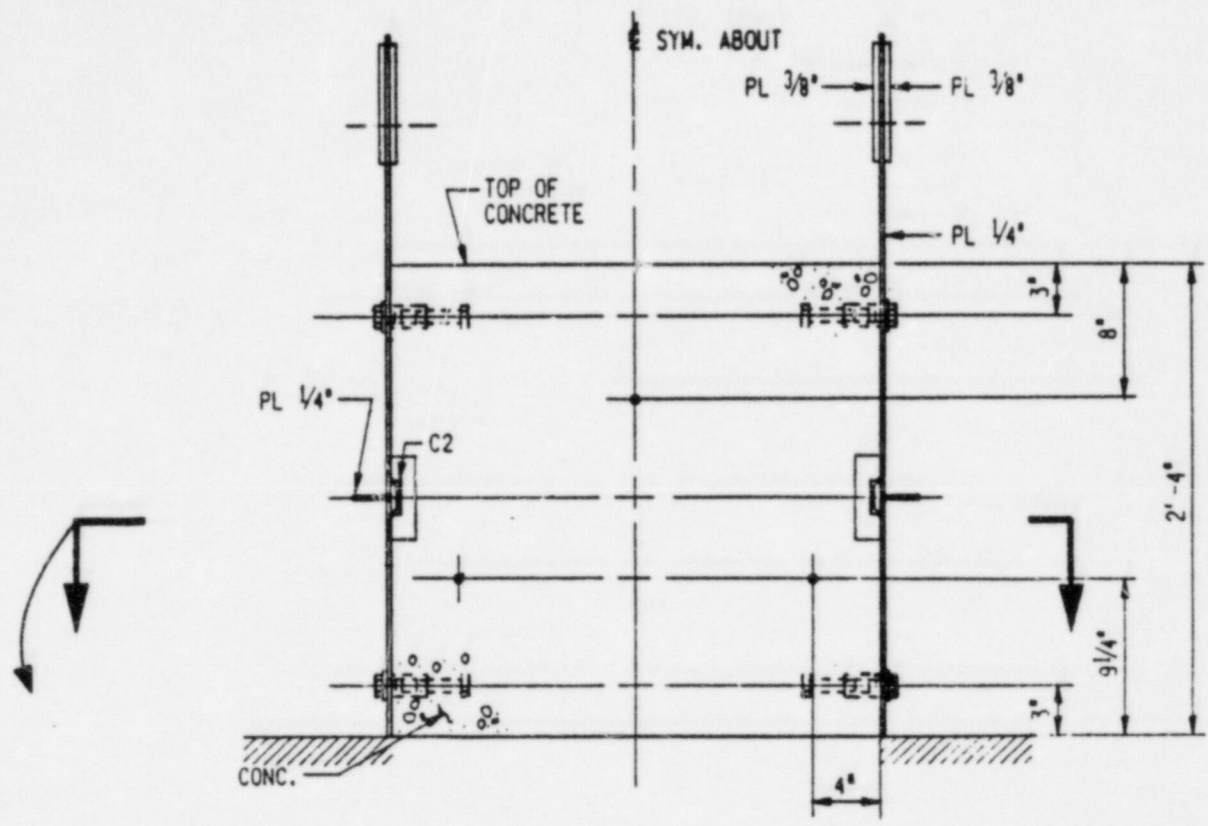
Data Point	Specimen I.A		Specimen I.B		Specimen II.A		Specimen II.B		Specimen III.A		Specimen III.B	
	Load (kips)	Displ. (inches)	Load (kips)	Displ. (inches)	Load (kips)	Displ. (inches)	Load (kips)	Displ. (inches)	Load (kips)	Displ. (inches)	Load (kips)	Displ. (inches)
0	0.000	0.0000	0.000	0.0000	0.000	0.0000	0.000	0.0000	0.000	0.0000	0.000	0.0000
1	1.489	0.0000	1.497	0.0000	2.979	0.0000	2.993	0.0000	2.979	0.0000	2.993	0.0000
2	2.979	0.0000	2.993	0.0000	6.187	0.0004	6.230	.0000	6.187	0.0000	6.230	.0000
3	4.583	.0000	4.612	0.0000	9.459	0.0006	9.430	0.0008	9.459	0.0005	9.430	0.0001
4	6.187	0.0004	6.230	.0000	12.583	0.0015	12.583	0.0018	12.583	0.0013	12.583	0.0009
5	7.823	0.0010	7.830	0.0001	15.738	0.0030	15.651	0.0021	15.738	0.0025	15.651	0.0016
6	9.459	0.0014	9.430	0.0002	18.807	0.0049	18.693	0.0034	18.808	0.0039	18.692	0.0030
7	11.021	0.0020	11.007	0.0006	21.829	0.0083	21.699	0.0060	21.829	0.0080	21.699	0.0040
8	12.583	0.0021	12.583	0.0007	24.850	0.0115	24.706	0.0088	24.850	0.0120	24.706	0.0081
9	14.161	0.0034	14.117	0.0015	27.957	0.0130	27.807	0.0118	27.958	0.0155	27.806	0.0120
10	15.738	0.0046	15.651	0.0016	31.065	0.0172	30.907	0.0148	31.065	0.0209	30.907	0.0163
11	17.273	0.0062	17.172	0.0018	34.086	0.0213	33.914	0.0183	34.087	0.0331	33.913	0.0193
12	18.808	0.0081	18.692	0.0026	36.201	0.0345	36.018	0.0213	37.108	0.0371	36.920	0.0308
13	20.318	0.0099	20.196	0.0063	37.107	0.0363	36.920	0.0273	38.627	0.0399	38.422	0.0326
14	21.829	0.0115	21.699	0.0081	38.627	0.0379	38.422	0.0298	40.147	0.0421	39.923	0.0350
15	23.339	0.0134	23.202	0.0096	40.146	0.0399	39.923	0.0311	15.696	0.1712	25.682	0.0365
16	24.850	0.0161	24.706	0.0112	41.665	0.0428	41.425	0.0332	14.897	0.2570	33.976	0.0366
17	26.404	0.0181	26.256	0.0132	43.185	0.0462	42.926	0.0355	15.145	0.2650	36.133	0.0371
18	27.958	0.0281	27.806	0.0147	44.711	0.0519	44.449	0.0376	14.662	0.2775	38.060	0.0382
19	26.359	0.0295	28.359	0.0156	46.237	0.0670	45.971	0.0381	14.914	0.2830	40.238	0.0403
20	26.496	0.0295	29.461	0.0163	47.763	0.0725	47.494	0.0391	14.778	0.2945	42.293	0.0427
21	26.857	0.0296	30.601	0.0173	49.289	0.0779	49.016	0.0412	2.669	0.2935	0.000	0.0236
22	26.982	0.0300	31.666	0.0187	50.850	0.0820	50.559	0.0431	8.869	0.2930	21.131	0.0245
23	27.342	0.0304	32.805	0.0199	52.411	0.0866	52.102	0.0444	8.869	0.2930	21.131	0.0246
24	27.467	0.0305	33.870	0.0223	51.607	0.0743	52.265	=>0.0450	14.672	0.2945	41.406	0.0430
25	23.544	0.0305	22.139	0.0267	44.289	0.0748	=>19.500	0.3365	15.289	0.2970	43.908	0.0476
26	31.065	0.0324	30.907	0.0279	46.428	0.0766	19.849	0.3645	15.390	0.2910	45.320	=>0.0530
27	34.087	0.0382	33.913	0.0307	0.000	0.0483	19.905	0.3700			=>19.470	0.1345
28	33.820	0.0507	35.880	0.0328	23.199	0.0520	7.110	0.3710				
29	32.767	0.0521	36.567	0.0324	43.209	0.0725	15.468	0.3710				
30	33.250	0.0527	38.762	0.0336	48.105	0.0775	20.563	0.3875				
31	33.609	0.0535	39.896	0.0346	53.003	0.0855	21.484	0.3920				
32	34.104	0.0541	42.132	0.0373	58.050	=>0.1100	22.414	0.3960				
33	34.364	0.0545	44.294	0.0407			23.394	0.3860				
34	34.632	0.0545	46.477	0.0600								
35	43.105	0.0574	51.256	0.0691								
36	49.500	=>0.0820	50.341	0.0698								
37	11.890	0.3640	19.682	0.0698								
38	15.437	0.3870	37.058	0.0707								
39	16.137	0.4015	42.723	0.0763								
40	15.717	0.4255	44.708	0.0660								
41	15.656	0.4415	46.170	0.0680								
42	15.907	0.4440	46.410	0.0680								
43	17.113	0.4760	51.881	=>0.0800								

=&gt; denotes a projected data point

TABLE B2-5 Summary of Shear Load versus Displacement Data for the Independent Steel Liner Plate LCC Tests

Point	Specimen S-I.A/B Load (kips) Displ. (inches)	Specimen S-II.A/B Load (kips) Displ. (inches)
0	0.125	0.0000
1	1.500	0.0000
2	2.500	0.0005
3	5.000	0.0030
4	7.500	0.0100
5	10.000	0.0180
6	12.500	0.0255
7	15.000	0.0340
8	17.500	0.0425
9	20.000	0.0515
10	22.500	0.0610
11	25.000	0.0710
12	27.500	0.0825
13	30.000	0.0970
14	32.500	0.1180
15	35.000	0.1445
16	37.500	0.1810
17	38.750	0.2105
18	40.000	0.2385
19	41.250	0.2660
20	42.500	0.3040
21	43.750	0.3530
22	45.000	0.4215
23	46.250	0.5250
24	47.500	0.6350
25	48.750	0.9175
26	49.250	0.11150
27	38.125	0.12030
28	33.250	0.12030
29	48.625	0.14140
30	47.125	0.15395
31	45.500	0.17175
32	41.750	0.18960
33	39.500	0.20725
34	36.750	0.22600
35	33.500	0.24450





TEST SPECIMEN FRONT ELEVATION

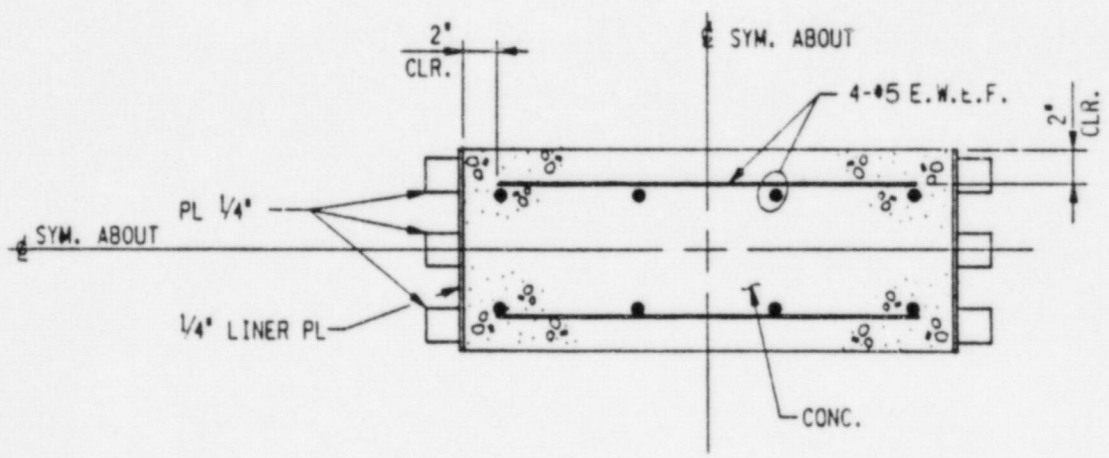


Figure B2-1 Composite Liner Plate LCC Specimen



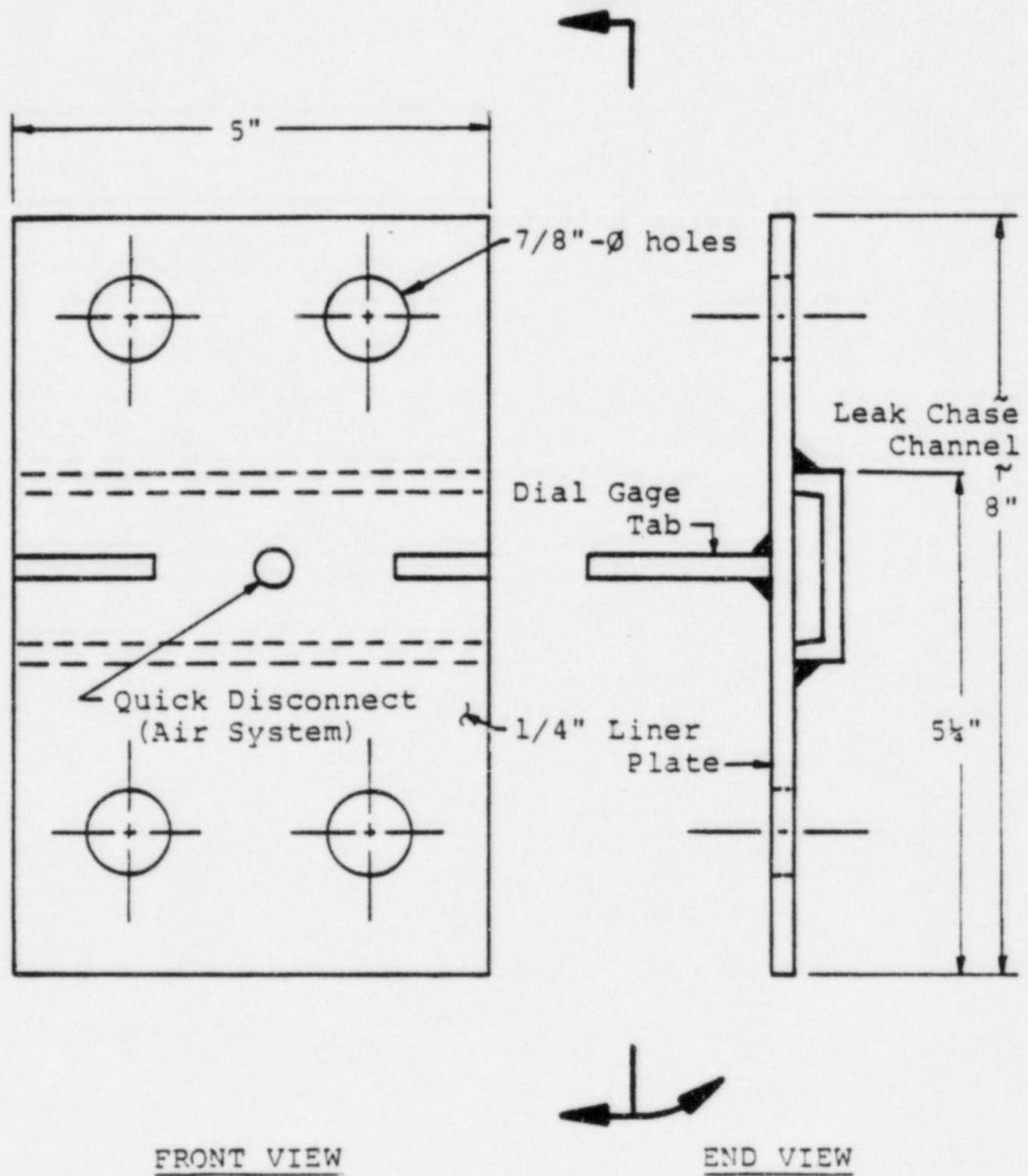


Figure B2-2 Independent Steel Liner Plate Leak Chase Channel Specimen

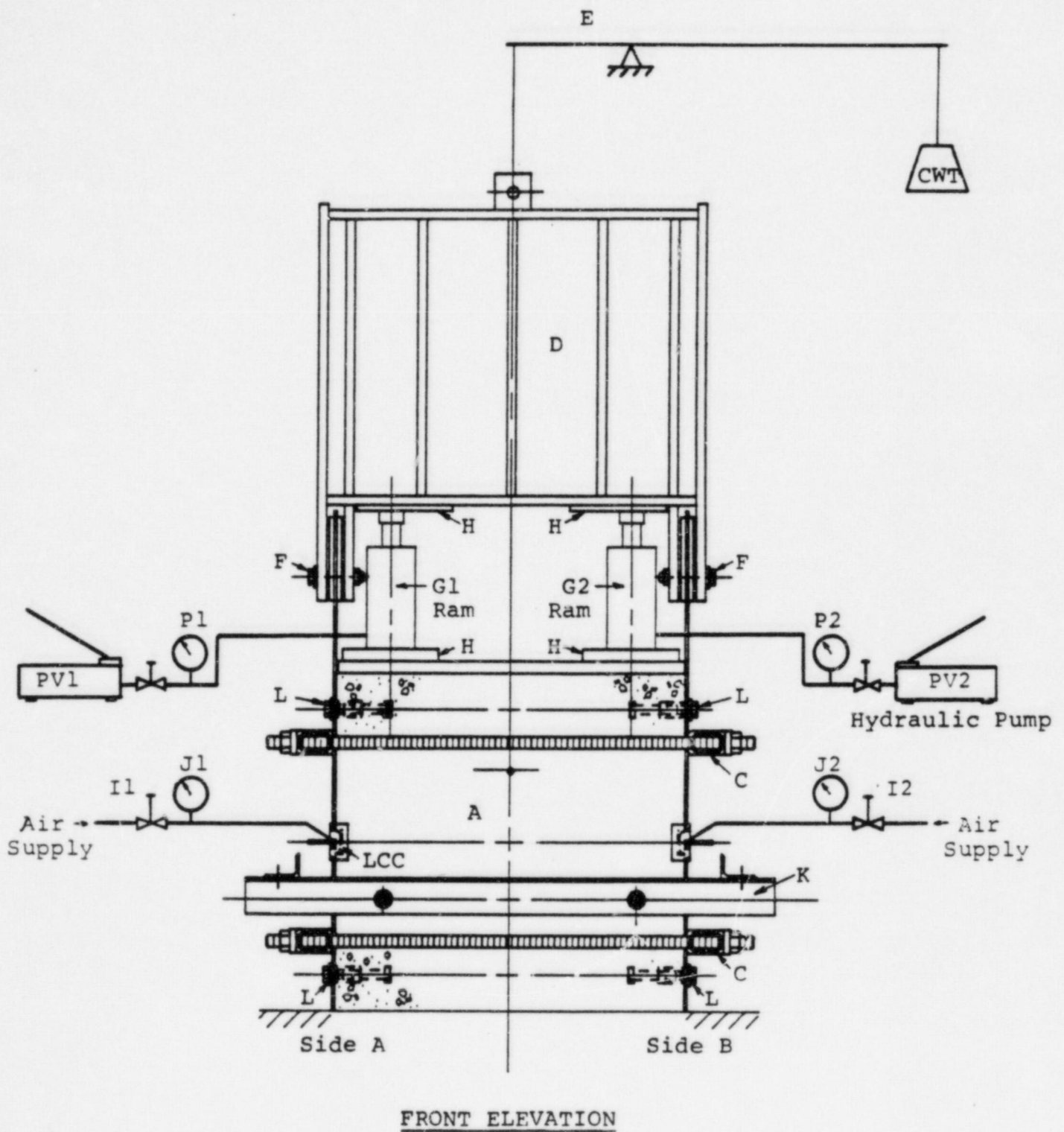


Figure B2-3 Composite Specimen Test Assembly including Pneumatic and Hydraulic Systems

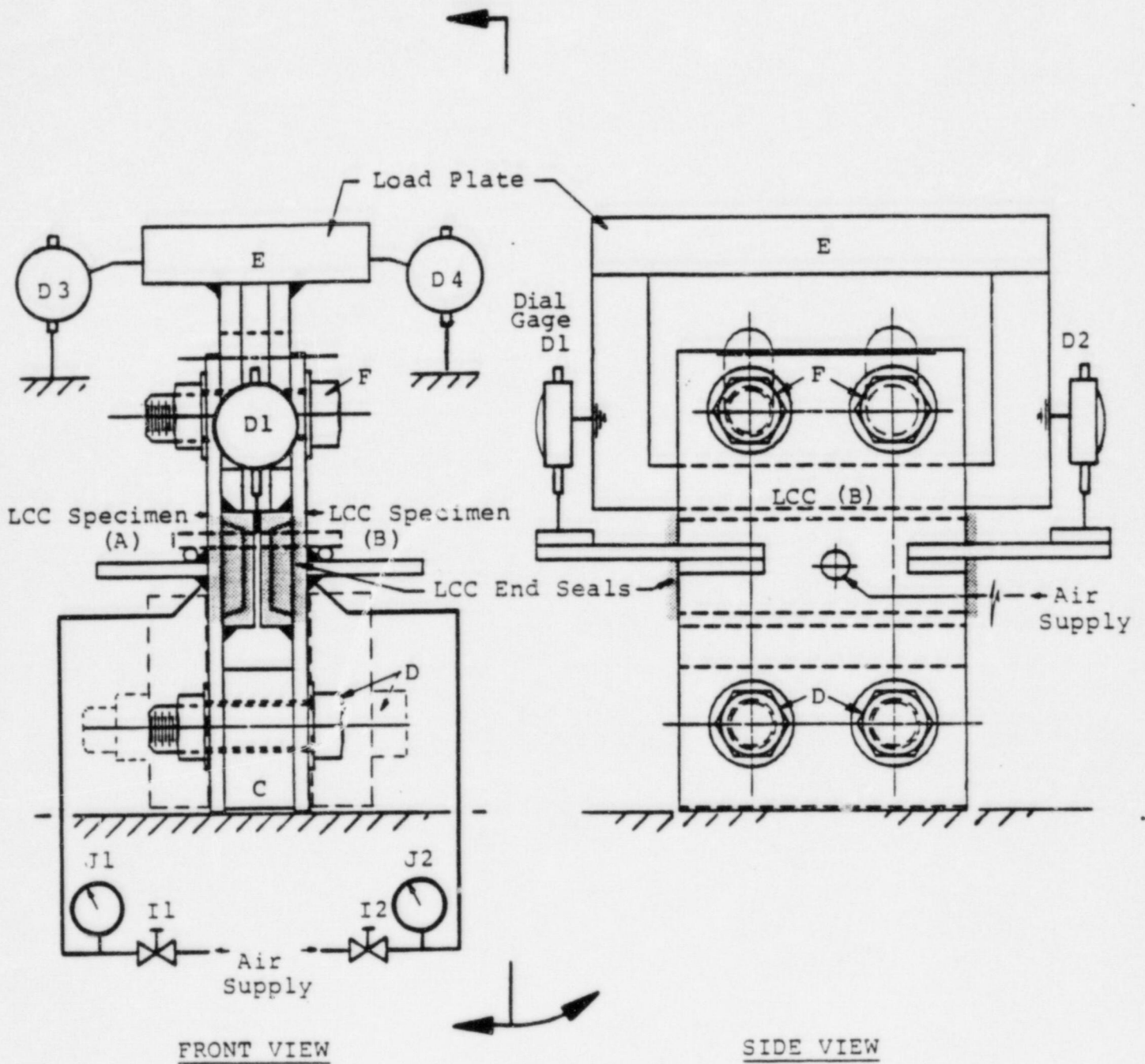


Figure B2-4 Test Assembly Including Pneumatic System and Dial Gage Arrangement for Independent Steel Specimen Tests

### B3.0 BILINEAR SPRING RATES

#### B3.1 COMPOSITE RESISTANCE FUNCTION

A combined plot of the composite test data from Table B2-4 for all tests (up to maximum load) is shown in Figure B3-1. The loads are plotted in terms of kips per inch (for a 1-inch specimen width). As can be seen from this figure, the composite behavior of the LCC specimens can be approximated by a bilinear resistance function.

The transition between the two response modes corresponds to the onset of cracking in the vicinity of the LCC bearing area. Initial cracking was first observed at loads between 21.7 to 24.9 kips (1.8 and 2 k/in. - see Table B2-3).

Examination of Figure B3-1 indicates the cracking likely started somewhat earlier at about 18 kips (1.5 k/in.). Therefore, for purposes of defining the two sections of the resistance function, the test data were partitioned at the 18 kip (1.5 k/in.) load level. Initial elastic stiffness was used to define the lower (elastic) limb and regression analysis was used to define the upper limb of the resistance function.

This resulted in the following equations defining the bilinear resistance function:

$$R = 553 X \quad R < 2.0 \quad \text{Eq B1}$$

$$R = 30.8 X + 1.888 \quad 2 < R < 4.13 \quad \text{Eq B2}$$

where

R = load resistance at displacement X (k/in.)  
X = shear displacement (inches)

The 2.0 and 4.13 k/in. limit on values of R correspond to the average elastic limit and peak load values for the 4.74 ksi test block concrete compressive strength.



### B3.2 STEEL LCC RESISTANCE FUNCTION

A plot of the test data from Table B2-5 for the independent liner plate LCC tests is shown in Figure B3-2. The loads in this figure are plotted in terms of kips per inch (for a 1-inch specimen width). The values shown are the average of both specimens in each of the two tests.

For each test the specimens remained linear up to loads of 6 to 7 k/in. after which P-delta effects started to introduce nonlinearities into the resistance functions. At higher load levels, local yielding in the LCC welds and flange-to-web corners introduced additional nonlinearity. Development of plastic section strengths, countered somewhat by strain hardening, caused further flattening of the curves as displacement levels were increased. At the average peak loads of 9.85 and 11.0 k/in. (for Tests I and II, respectively), deformation control shifted from the LCC (welds and corner section plasticity) to the 1/4-inch liner plate plastic hinge formation in the liner plate sections above and below the LCC. At this point, P-delta effects on the 1/4-inch liner plate sections resulted in diminishing assembly load resistance as deformations were increased.

To minimize the plate section P-delta effects, a 1-inch-thick steel retainer block was bolted to the bottom the the test assembly in Test II (shown by dashed lines in Figure B2-4). The 1 x 3-1/2 x 5-inch block was secured to the assembly by 3/4-inch high strength bolts (Item D in Figure B2-4). This resulted in slightly higher stiffness and peak resistance in Test II. This was considered more representative of the in-plane LCC sections. Therefore, the data from Test II (average of values from specimens S-IIA and S-IIB) were used for development of steel LCC section resistance functions.

The resistance function was idealized as an elastic-perfectly-plastic system as shown in Figure B3-2. The upper limit value of 10 k/in. was used (instead of the peak value of 11 k/in.) to achieve an approximate strain energy balance. The stiffness corresponds to the average initial linear range stiffness. Considering that the plastic resistance is controlled primarily by the yield strength of the LCC channel section steel, results in the following equations defining the bilinear resistance function:

$$R = 720 X \qquad R \leq \frac{f_y}{6.16} \qquad \text{Eq B3}$$

$$R = \frac{f_y}{6.16} \qquad X \geq \frac{f_y}{4435} \qquad \text{Eq B4}$$

where

R = load resistance at displacement X (kips)  
X = shear displacement (inches)

### B3.3 MATERIALS PROPERTIES EFFECTS

The stiffness values reflected in Equations B1 and B2 are a function of both concrete and steel stiffness (for a 1-inch wide strip). The linear limit is a function of the square root of the concrete strength, while the ultimate load is a direct function of the concrete compression strength. The stiffness values in both ranges are a function of the concrete elastic modulus which, in turn, is a function of the square root of the concrete compressive strength. The stiffness contribution of the LCC steel section is defined by Equation B3 and is invariant with steel strength values. The upper limit steel LCC load resistance is, however, a direct function of the LCC section steel yield strength,  $f_y$ .

The foregoing relationships enable development of resistance function formulas to account for variations in both steel and

concrete materials properties. The following relationships reflect a 1-inch-wide strip.

Elastic limit ( $R_Y$ ):

$$R_Y = 2 \sqrt{\frac{f_c}{4.74}}$$

$$R_Y = \sqrt{\frac{f_c}{1.185}}$$

$$R_Y \leq \frac{f_y}{6.16}$$

Eq B5

where

$f_c$  = concrete compressive strength (ksi)

Ultimate strength ( $R_U$ ):

$$R_U = 4.13 \frac{f_c}{4.74}$$

$$R_U = \frac{f_c}{1.148}$$

$$R_U \leq \frac{f_y}{6.16}$$

Eq B6

Stiffness variation with concrete strength:

$$\frac{1}{K_c} + \frac{1}{K_s} + \frac{1}{K_t}$$

Eq B7

or

$$K_t = \frac{K_c K_s}{K_c + K_s}$$

or

$$K_c = \frac{K_s K_t}{K_s - K_t}$$

where

$K_c$  = concrete stiffness (k/in.)

$K_s$  = steel LCC section stiffness (k/in.)

$K_t$  = combined concrete and steel LCC stiffness (k/in.)

From test data for  $f_c = 4.74$  ksi and  $f_y = 61.6$  ksi for a 1-inch-wide strip:

$$K_t = 553 \text{ k/in.}$$

$$R < R_y = 2 \text{ k}$$

$$K_t = 30.8 \text{ k/in.}$$

$$R_y \leq R \leq R_u$$

$$R_y = 2 \text{ k}$$

$$R_u = 4.13 \text{ k} \\ (\text{k} = \text{kips})$$

$$K_s = 720 \text{ k/in.}$$

$$0 < R < R_u$$

$$R_u \leq \frac{f_y}{6.16}$$

Substitution of these  $K_t$  and  $K_s$  values into Equation B7 results in the following isolated concrete elastic stiffness values.

$$K_c = 2384 \text{ k/in.}$$

$$0 < R \leq R_y$$

$$K_c = 32.18 \text{ k/in.}$$

$$R_y \leq R \leq R_u$$

The concrete stiffness modified to reflect compression strength variation would be:

$$K_c = 2384 \sqrt{\frac{f_c}{4.74}}$$

$$K_c = 1095 \sqrt{f_c}$$

$$0 < R_y < R$$

Eq B8

$$K_c = 32.18 \sqrt{\frac{f_c}{4.74}}$$

$$K_c = 14.78 \sqrt{f_c}$$

$$R_y \leq R \leq R_u$$

Eq B9

$R_y$  and  $R_u$  are defined by Equations B5 and B6.

where

$f_c$  = concrete compressive strength (ksi)



Defining the initial elastic stiffness as  $K_a$  and the upper limb stiffness as  $K_b$  (such as in Figure 7-2), the LCC resistance function can be defined by the following relationships:

$$R = K_a X \qquad 0 \leq R \leq R_y \qquad \text{Eq B10}$$

$$R = K_b X + 1.888 \sqrt{\frac{f_c}{4.74}}$$

$$R = K_b X + 0.867 \sqrt{f_c} \qquad R_y \leq R < R_u \qquad \text{Eq B11}$$

Letting  $K_t$  equal  $K_a$  or  $K_b$ , and substituting the proper values of  $K_c$  and  $K_s$  into Equation B7,  $K_a$  and  $K_b$  are defined as follows:

$$K_a = \frac{788,400 \sqrt{f_c}}{1095 \sqrt{f_c} + 720} \qquad \text{Eq B12}$$

$$K_b = \frac{10,642 \sqrt{f_c}}{14.78 \sqrt{f_c} + 720} \qquad \text{Eq B13}$$

$$K_b = 0 \text{ if } R_y = \frac{f_y}{6.16} \qquad \text{Eq B14}$$

$$\text{or } R_u = \frac{f_y}{6.16}$$

Substitution of the values of  $K_a$  and  $K_b$  from Equations 12 through 14 into Equations B10 and B11 and observing the limits of  $R_y$  and  $R_u$  as defined by Equations B5 and B6, LCC load versus displacement functions can be defined for various combinations of concrete compressive and steel yield strengths.

Values of yield and ultimate displacement ( $X_y$  and  $X_u$ ) can also be obtained from Equations B10 and B11 by substitutions  $R_y$  or  $R_u$  for  $R$  and solving for  $X_y$  or  $X_u$ . In cases where  $K_b$  is equal to zero (capacity controlled by LCC steel yield

strength,  $R_u = f_y/6.16$ ) the value of  $X_u$  can be determined as follows:

$$X_u = \frac{R_u}{K_{ca}} + 0.095 \quad \sqrt{\frac{f_c}{1.185}} > R \quad \text{Eq B15}$$

$$R_u = \frac{f_y}{6.16}$$

$$X_u = \frac{R_y}{K_{ca}} + \frac{R_u - R_y}{K_{cb}} + 0.095 \quad \sqrt{\frac{f_c}{1.185}} < R_u < \frac{f_c}{1.148} \quad \text{Eq B16}$$

$$R_u = \frac{f_y}{6.16}$$

where

$X_u$  = ultimate limits for displacement (inches)  
 $K_{ca}$  = concrete stiffness as defined by Equation B8 (k/in.)  
 $K_{cb}$  = concrete stiffness as defined by Equation B9 (k/in.)

The foregoing relationships were used to determine the LCC spring element properties in Table B3-1 from the steel and concrete strength properties contained in Table 5-2 and 5-3. The LCC properties are also listed in Table 7-1 along with those for other liner plant elements.

TABLE B3-1 - LCC BILINEAR SPRING PROPERTIES(1)

<u>Strength Range</u>	LCC	(2)						
	$f_y$ (ksi)	$R_{us}$ (k)	$f_c$ (ksi)	$R_o$ (k)	$R_y$ (k)	$R_u$ (k)	$X_y$ (in.)	$X_u$ (in.)
Min	36	5.84	6.0	2.123	2.261	5.226	0.003983	0.0900
Mean	45	7.31	8.5	2.528	2.716	7.31 (steel limit)	0.004622	0.1176
Max	61.6	10.0	11.0	2.876	3.113	9.582	0.005181	0.1461
Spec	36	5.84	5.0	1.939	2.055	4.355	0.003694	0.07646
	$f'_c$ (ksi)	$K_a$ (k/in.)	$K_b$ (k/in.)					
Min	6.0	567.6	34.47					
Mean	8.5	587.5	40.66					
Max	11.0	600.9	45.90					
Spec	5.0	556.4	31.60					

(1) See text for definition of terms.

(2)  $R_{US}$  is the ultimate load capacity determined by steel yield strength,  $f_y$ .

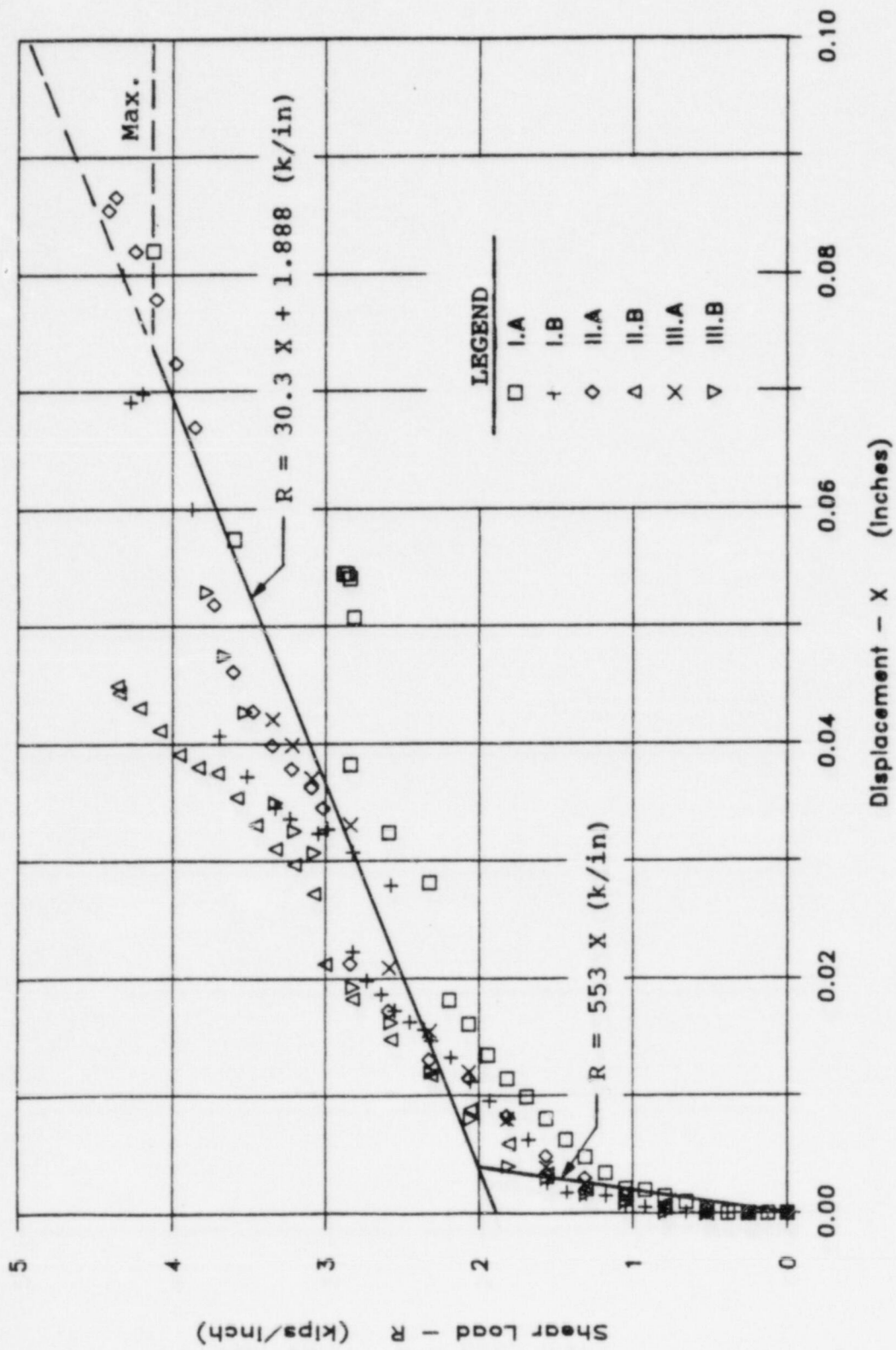


Figure B3-1 Combined Plot of Composite Test Data for All Tests up to Maximum Load



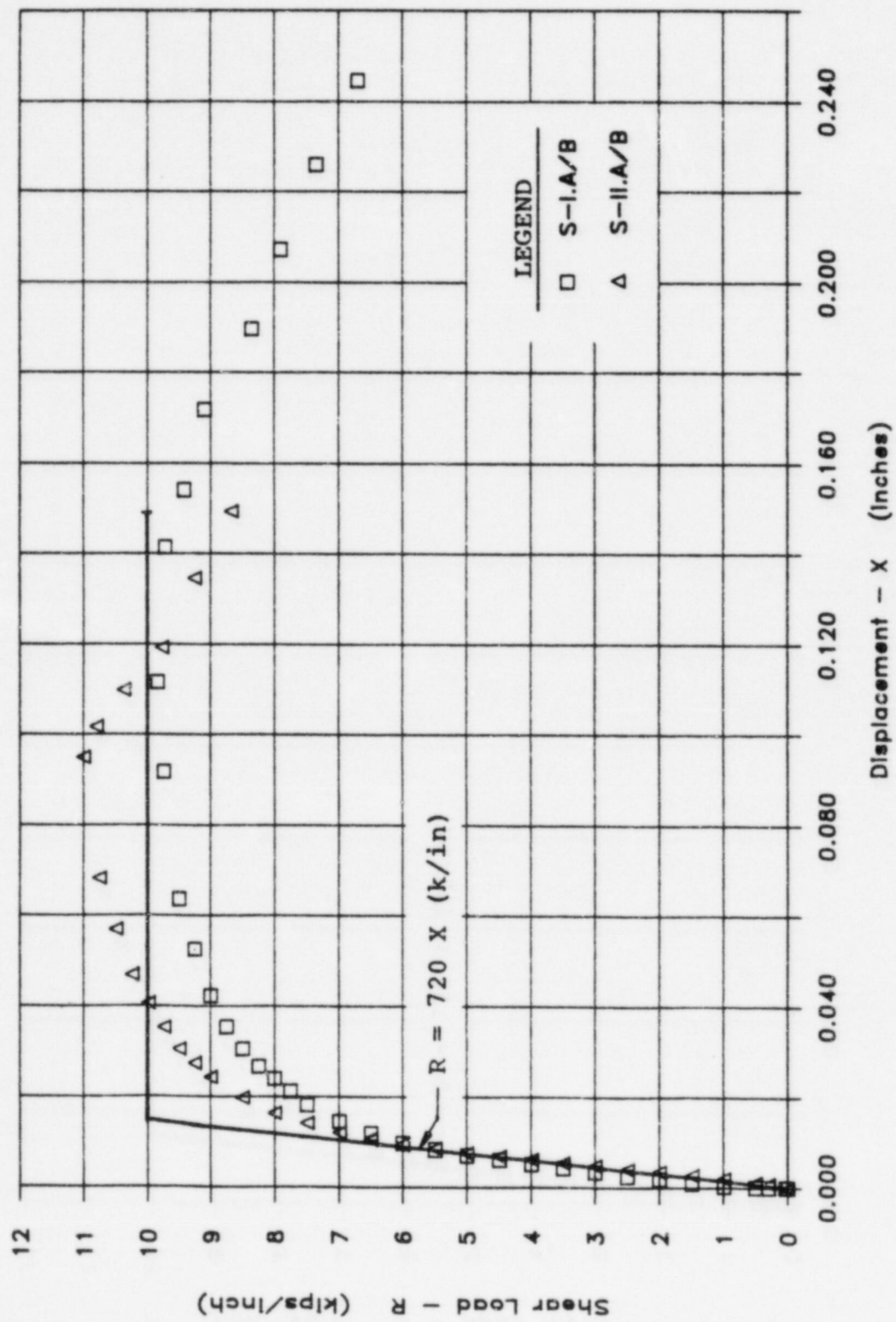


Figure B3-2 Combined Plot of Load versus Displacement Data for Independent Steel Liner Plate LCC Tests